

Toward Nonaqueous Alkanolamine-Based Carbon Capture Systems: Parameterizing Amines, Secondary Alcohols, and Carbon Dioxide-Containing Systems in s-SAFT- γ Mie

Alexander Schulze-Hulbe, Fariborz Shaahmadi, Andries J. Burger, and Jamie T. Cripwell*



Cite This: *Ind. Eng. Chem. Res.* 2023, 62, 14061–14083



Read Online

ACCESS |

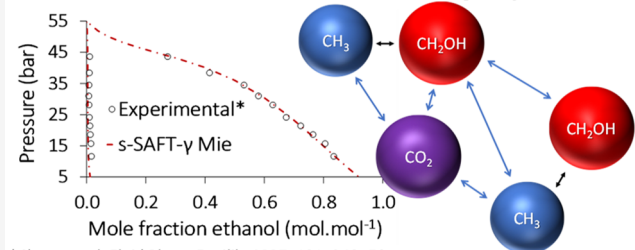
Metrics & More

Article Recommendations

Supporting Information

ABSTRACT: Replacement of aqueous alkanolamine-based carbon capture fluids with nonaqueous alternatives may be a promising route to reduce the energy requirements of current postcombustion carbon capture processes. In line with this, the s-SAFT- γ Mie predictive group contribution Equation of State is developed toward a description of the thermodynamic properties of nonaqueous alkanolamine-based carbon capture systems in this work. A consistent and systematic methodology is used to develop s-SAFT- γ Mie group interaction parameters required for modeling these systems. This entails extending the model to the primary amine ($\text{CH}_2\text{NH}_2/\text{NH}_2$) and secondary alcohol (CHOH) groups, as well as their interactions with the *n*-alkane (CH_2 and CH_3) and primary alcohol ($\text{CH}_2\text{OH}/\text{OH}$) groups. Parameters were also developed for the interactions of CO_2 with the *n*-alkane, primary alcohol, and secondary alcohol groups, respectively. The model, with its active parameter sets, generally provides a robust description of the phase equilibria of the systems considered. This renders the developed parameters suitable for expanding the model to ternary-component alkanolamine-based nonaqueous carbon capture systems in further work.

s-SAFT- γ Mie: predictive EoS that describes systems as interactions between functional groups



*Chang et al. *Fluid Phase Equilib.* 1997, 131, 243–58.

1. INTRODUCTION

1.1. Nonaqueous Carbon Capture. An estimated 25% of global CO_2 emissions arise from industrial processes.¹ Accordingly, decarbonizing the industrial sector will play a key role in meeting emissions targets,² and thereby mitigating the deleterious effects of climate change. Capture and storage of CO_2 emitted from large point sources is a feasible option for the decarbonization of several emissions-intensive industries,² such as the cement industry.³ The application of carbon removal technologies is particularly promising in the refining and petrochemical industries, as the cost thereof is arguably negligible compared to market fluctuations.² Looking beyond the industrial sector, CO_2 capture and storage (CCS) is required for purifying biogas.⁴ Notably, it has also been used for the decarbonization of fossil-fuel fired power plants: The only commercial-scale carbon capture processes have been implemented at coal power plants.⁵ As such, CCS may provide an important step toward generating low-carbon electricity.

A popular approach to CCS is to remove CO_2 from fossil fuel combustion effluent gases. Of these postcombustion CCS technologies, chemical absorption of CO_2 is the most mature one compared to its competitors.^{6,7} Conveniently, chemical absorption processes can be retrofitted to existing power plants.⁸ This arguably increases the ease of implementation of these processes. In typical chemical absorption CCS processes, the CO_2 -containing flue gas stream is contacted with an

aqueous solution of alkanolamines. The alkanolamines react with the CO_2 , thereby capturing it in the liquid phase and purifying the gas stream. In-depth discussions of chemical absorption for postcombustion CCS can be found in the works of Bui et al.⁹ and Liang et al.⁷

Despite the maturity of alkanolamine-based carbon capture, a major challenge faced by the technology is its high energy demand.^{5,10–12} Indeed, overcoming these high energy requirements is essential for wide-scale adoption of absorption-based CCS processes.¹³ This is an important step in realizing the technology's carbon capture potential. The largest contributor to the cost of absorption-based carbon capture, and the subsequent compression of CO_2 , is the energy required for releasing (desorbing) the CO_2 after absorption by the alkanolamine solvent.¹⁴ This energy must be significantly reduced to achieve substantial cost reductions in absorption-based carbon capture,¹⁴ and is one of the most critical parameters for process optimization.¹¹ Solvent regeneration entails heating and vaporizing the solvent, as well as releasing

Received: May 8, 2023

Revised: July 31, 2023

Accepted: August 14, 2023

Published: August 25, 2023



the CO₂ bound within it. Particularly the heating requires significant energy input, owing to water's very high heat capacity. Accordingly, it is intuitive that water should be replaced with an organic cosolvent.¹² Organic cosolvents not only have lower heat capacities compared to water, but also lower heats of vaporization.^{11,15} In a computational study, Bahamon et al.¹⁶ found that several nonaqueous alkanolamines show reduced energy consumption relative to their aqueous counterparts. This agrees with similar work by Alkhatab et al.¹⁷ Wanderley et al.¹⁸ maintain that energy costs associated with vaporization (and energy duties overall) can certainly be reduced by using nonaqueous cosolvents.¹⁸

However, there are certain drawbacks associated with the use of nonaqueous carbon capture fluids: Reduced heat transfer will likely necessitate more expensive heat exchangers,¹⁸ and CO₂ removal is more inefficient for nonaqueous water alternatives,^{16,17,19} although this may not always be the case.^{16,18} Mathias et al.²⁰ point out that process intensification and process integration may be able to compensate for the disadvantages of nonaqueous systems. Moreover, Bahamon et al.¹⁶ note that a trade-off can be struck between CO₂ removal efficiency and energy requirements.

On the other hand, a nonaqueous process fluid can be used to lower the regeneration temperature.¹¹ Lower temperatures may reduce some serious process issues: solvent decomposition,^{21–25} evaporation,^{21–24} and equipment corrosion,^{21–23,25} providing further motivation for using organic cosolvents in chemical absorption carbon capture processes.

Against this background, reliable and accurate thermodynamic modeling of both aqueous and nonaqueous alkanolamine-based CCS is essential to ensure appropriate design and fair comparison between systems. In pursuit of this goal, this work specifically focuses on improving the thermodynamic modeling of nonaqueous alkanolamine-based systems.

1.2. SAFT and the Group Contribution Approach. The Statistical Associating Fluid Theory (SAFT) Equations of State (EoSs) are an appropriate family of thermodynamic models for use in modeling thermodynamic properties of carbon capture systems. Given that they were developed on the basis of Wertheim's thermodynamic perturbation theory,^{26–29} they are firmly grounded in statistical mechanics. In the SAFT framework, the residual Helmholtz free energy of a thermodynamic system (A^{res}) is determined as a summation of several types of interactions between molecules consisting of chain-like segments. This is shown in eq 1.

$$A^{\text{res}} = A^{\text{hard sphere}} + A^{\text{dispersion}} + A^{\text{chain}} + A^{\text{association}} \quad (1)$$

where $A^{\text{hard sphere}}$ and $A^{\text{dispersion}}$ are hard sphere repulsive and dispersive interactions between the segments, A^{chain} refers to chain formation between the segments to form molecules, and $A^{\text{association}}$ refers to highly directional association interactions between molecules. Given that eq 1 is a summation, additional terms can be added to account for all manner of intermolecular interactions that deviate from ideal gas behavior. Existing terms can also be modified, enabling continuous model improvement. This renders SAFT EoSs highly flexible, enabling them to model a wide range of complex thermodynamic systems. These include polymers,^{30–37} electrolytes,^{38–46} and fluids exhibiting hydrogen bonding.^{47–51} Their significant modeling capabilities render SAFT EoSs well-suited to reproducing the challenging thermodynamic behavior found in alkanolamine/cosolvent/CO₂ systems.

A noteworthy SAFT variant is SAFT-VR Mie.⁵² "VR Mie" refers to the realistic Mie potential of variable range the EoS uses to model intermolecular interactions. The Mie potential enables the model to provide an accurate description of thermodynamic properties beyond phase equilibria, like the liquid isobaric heat capacity.^{52–54} Moreover, the use of SAFT-VR Mie's sophisticated dispersion term (a third-order perturbation expansion) has also been attributed to its improved description of isobaric heat capacities.⁵⁵ Furthermore, SAFT-VR Mie is capable of an improved description of the critical region compared to its contemporaries.^{52,53,56} Detailed descriptions of SAFT-VR Mie are provided in the works of Dufal, Lafitte and co-workers.^{52,56,57} For further details regarding SAFT EoSs more broadly, the reader is referred to the reviews by Müller and Gubbins⁵⁸ and Tan et al.,⁵⁹ as well as Chapter 8 in Kontogeorgis and Folas.⁶⁰

Pertinently, approaches have also been developed that enable SAFT EoSs to predict a range of properties for species for which no data are available. One such predictive modeling approach is to use correlations for model parameters that depend on the molecular weight of different species.^{61–63} A more popular approach is the group contribution (GC) method, in which thermodynamic systems are described in terms of interactions between their constituent functional groups as opposed to interactions between molecules. For instance, for *n*-propane, attractive and repulsive interactions do not occur between molecules (C₃H₈), but rather between the constituent functional groups, CH₃ and CH₂. Figure 1

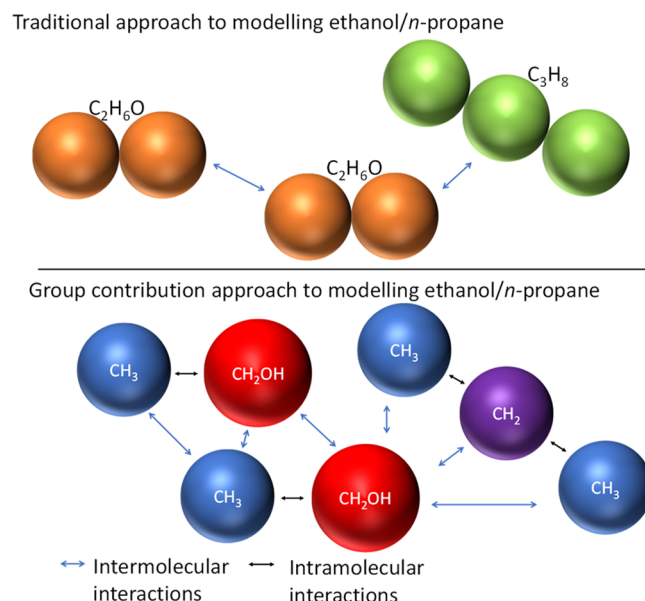


Figure 1. Illustration of the difference between the traditional and group contribution approaches to thermodynamic modeling.

illustrates the difference between the traditional and group contribution approaches to thermodynamic modeling. Shaah-madi et al.⁶⁴ provide a comprehensive review of GC approach SAFT EoSs.

A noteworthy GC approach SAFT variant is the SAFT- γ Mie EoS.⁶⁵ This is the implementation of the powerful SAFT-VR Mie EoS in a GC framework. As summarized by Haslam et al.,⁶⁶ SAFT- γ Mie has been parametrized for a wide range of thermodynamic systems of industrial relevance. These include

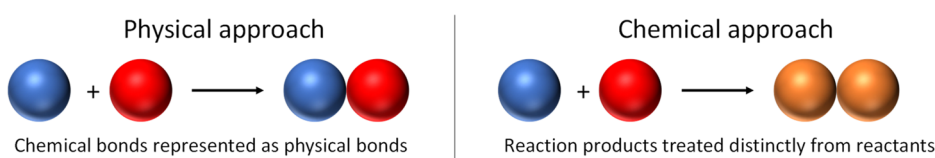


Figure 2. Illustration of the difference between the physical and chemical approaches to modeling reaction equilibria.

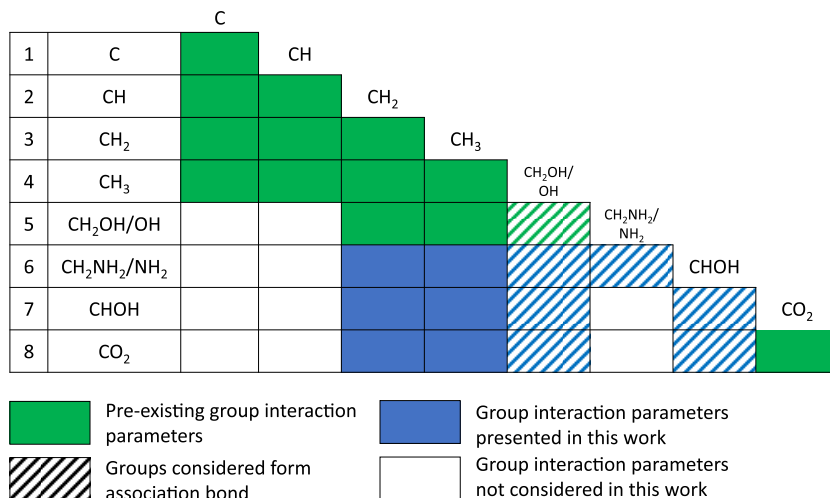


Figure 3. Pre-existing s-SAFT- γ Mie interaction parameters and those discussed in this work.

aqueous pharmaceutical substances,^{67,68} electrolytic solutions,⁶⁶ and aqueous alkanolamine systems.⁶⁹

Despite its many successful implementations, SAFT- γ Mie cannot distinguish between structural isomers. Accordingly, the model has recently been modified to account for the nuanced differences between isomers, yielding the structural (s)-SAFT- γ Mie EoS.⁷⁰ It was shown that the accuracy of s-SAFT- γ Mie rivals that of SAFT- γ Mie for linear *n*-alkanes, and that it is capable of accurate distinction of the isomers of branched species.⁷⁰ The model was subsequently extended to primary alcohols,⁷¹ where it was shown that s-SAFT- γ Mie's descriptions of primary alcohols and their mixtures with *n*-alkanes are comparable to those obtained with SAFT- γ Mie. The s-SAFT- γ Mie model parameters as well as the combining rules used are discussed in previous work.⁷¹

GC modeling approaches are valuable to carbon capture process designers: They can significantly narrow the time and resources expended during alkanolamine/cosolvent selection, as only the promising alkanolamines and cosolvents identified with these methods need to be investigated experimentally. The works of Papadopoulos et al.⁶ and Papadopoulos et al.⁷² illustrate how SAFT EoSs that utilize the GC modeling approach can be a powerful tool for solvent screening.

1.3. SAFT Modeling of Alkanolamine-Based Carbon Capture Systems. Much work has been done on modeling alkanolamine-based carbon capture systems with SAFT-type EoSs. Of note is the work of Mac Dowell and co-workers^{73–75} with the SAFT EoS for potentials of variable range ("SAFT-VR").⁷⁶ This EoS uses a square well intermolecular potential and is a predecessor of SAFT-VR Mie. Mac Dowell and co-workers^{73–75} represent the chemical reaction equilibria between CO₂ and the alkanolamine as highly directional and short-ranged intermolecular interactions (association bonds). An alternative to this so-called "physical" approach is the "chemical" one, in which key chemical reaction products

(bicarbonate and carbamate),^{77,78} as well as hydrogen bonded molecules, are treated distinctly from unreacted or unbonded molecules. The difference between these approaches is illustrated in Figure 2.

Notably, it has been shown that physical models rooted in statistical mechanics are equivalent to chemical models if the reaction products do not form significantly different species,⁷⁹ lending credence to this approach. Further, a key advantage of the physical approach is that it does not require prespecifying the reaction products or equilibrium constants, reducing the models' dependence on experimental data.⁷⁷ As these are unknown for many systems, this approach results in greatly enhanced predictive capabilities, providing SAFT EoSs with a significant advantage over other modeling approaches (e.g., models based on excess Gibbs free energy, like NRTL⁸⁰).

Although the physical approach only predicts the formation of the main reaction products (viz., carbamate and bicarbonate), it can provide an estimate of the relative proportions thereof. This ability to incorporate reaction equilibria and estimate key reaction product concentrations is a noteworthy feature of using SAFT-type EoSs for modeling alkanolamine-based carbon capture systems. Owing to its success, the physical approach to modeling reaction equilibria in alkanolamine/water/CO₂ systems has also been used by successors of SAFT-VR, namely, SAFT- γ SW (square well)⁷⁷ and SAFT- γ Mie.⁷⁸ Moreover, the approach has also been used with the soft-SAFT EoS.^{81–83}

Although significant effort has been directed toward modeling ternary alkanolamine/water/CO₂ phase equilibria within the SAFT framework,^{73–75,77,78,81–87} much less attention has been paid to nonaqueous carbon capture cosolvents, despite their potential advantages over aqueous ones. To the authors' best knowledge, only the soft-SAFT EoS^{88–90} has been applied to modeling alkanolamine/organic

cosolvent/CO₂ systems in the work of Alkhatib, Bahamont, and co-workers.^{16,17,91}

1.4. Aim and Objectives. Given the promise of non-aqueous carbon capture systems, and the lack of attention these systems have received from the thermodynamic modeling community, the aim of this work and of subsequent work is to develop s-SAFT- γ Mie group interaction parameters for modeling the thermodynamic properties of these fluids.

s-SAFT- γ Mie functional group interaction parameters will be regressed for the groups that constitute alkanolamine/organic cosolvent/CO₂ systems, where it can be inferred from Figure 3 that the EoS is still in its infancy: Parameters for a wide range of interactions must be developed before ternary alkanolamine/organic cosolvent/CO₂ systems can be modeled.

Accordingly, the parametrization will be performed in two parts. In the first, the required interaction parameters will be regressed from pure-component and binary mixture subsystems. In the second, the parameters thus obtained will be transferred to ternary systems, and remaining interactions will be parametrized. This paper constitutes part I of the model parametrization. The interaction parameters discussed in this paper pertain to primary amines, secondary alcohols, alkanolamines as well as *n*-alkane/CO₂, primary alcohol/CO₂, and secondary alcohol/CO₂ systems.

A myriad of approaches can be followed in developing parameters for s-SAFT- γ Mie, and group contribution SAFT models more broadly. Yet there is no standardized approach to the development and implementation of thermodynamic models,⁹² meaning that no set parametrization methodology exists. This is particularly evident in the wide variety of property types that have been included in the parametrization: These include mixture properties like excess enthalpy^{65,93–95} and binary VLE^{96–100} as well as derivative properties like heat of vaporization^{54,98,101,102} and speed of sound.^{51,103,104} There is no consensus regarding what approach should be followed. The lack of standardization is a cause for serious concern for industrial practitioners⁹² and naturally presents a hurdle to the industrial use of thermodynamic models. Considering this, a secondary aim of this work is to provide an example of how group contribution SAFT models can be parametrized consistently and systematically in the context of nonaqueous alkanolamine-based carbon capture systems. The methodology thus employed follows that used in our previous work⁷¹ for developing s-SAFT- γ Mie parameters for primary alcohols.

2. METHODOLOGY

2.1. Determining Functional Groups and Choosing Association Sites. Within the GC approach SAFT EoSs, the structure of functional groups used must be defined. Wu and Sandler¹⁰⁵ suggest the requirement that the net charge and geometry of a group should not depend on the molecule of which it is a part. Noting the effect of the OH group's charge on the adjacent CH₂ group, these authors have suggested a larger primary alcohol group over a smaller one.¹⁰⁵ Therefore, the CH₂OH group was used for primary alcohols.⁷¹ Similar choices are made for the functional groups considered in this work. However, with the future development of the model in mind, it may be sensible to use smaller groups. These smaller groups provide the model with increased flexibility, more readily facilitating the treatment of branched alkanolamines in further work. Accordingly, the performance of smaller groups is considered in this work. The functional group definitions are shown in Table 1.

Table 1. Functional Group Definitions and Their Respective Numbers of Segments (v_k^*)

group	number of segments (v_k^*)	
primary alcohol (coarse-grained)	CH ₂ OH	2
primary alcohol (fine-grained)	OH	1
primary amine (coarse-grained)	CH ₂ NH ₂	2
primary amine (fine-grained)	NH ₂	1
secondary alcohol	CHOH	2
carbon dioxide	CO ₂	2

For species consisting only of a single functional group, such as CO₂, s-SAFT- γ Mie is mathematically identical to SAFT- γ Mie. Therefore, the SAFT- γ Mie CO₂ parameters developed by Papaioannou et al.⁹⁵ were used in this work. These provide accurate descriptions of CO₂ pure-component properties, as illustrated by those authors.⁹⁵

Moreover, the number and type of sites at which the highly directional association bonds can occur must also be chosen for each functional group. Primary amines have been modeled with one electron donor ("e") and two electron acceptor ("H") sites,^{49,74,83,106–109} or one e-site and one H-site.^{107,109–111} The former is referred to as a 3-site association scheme, whereas the latter is a 2-site scheme. Both options are illustrated in Figure 4.

Similarly, secondary alcohols have been modeled with two e-sites and one H-site^{66,112,113} or one e-site and one H-site.^{51,114–116} These options are listed in Figure 5. In accordance with the methodology employed previously,⁷¹ both possibilities are considered for primary amines and secondary alcohols.

Unlike amines or alcohols, CO₂ does not form association bonds in its pure form. However, it forms association bonds (i.e., it cross-associates) with other associating species. This is evidenced by the Lewis acid–base interactions observed between CO₂ and methanol.¹¹⁷ Failure to account for cross-association between CO₂ and alcohols can lead to the prediction of false liquid–liquid phase splits.^{118–120} Accordingly, cross-association will be accounted for in this work. NguyenHuynh et al.¹¹⁹ as well as Björner and Kontogeorgis¹²⁰ have used two cross-association ("X") sites to model CO₂. These sites can act as both positive and negative sites, depending on which type of site they interact with on unlike molecules. However, Smith et al.¹¹⁸ have pointed out that CO₂ acts as an electron acceptor. Accordingly, it may be sensible to treat CO₂ as having two positive ("H") sites. The two options are shown in Figure 6. Although both the cross-association model and the two H-sites model perform similarly in the SAFT-VR Mie context,¹¹⁸ both schemes will be investigated for suitability in this work.

2.2. Parameter Fitting Procedure. Pure-component vapor pressure and saturated liquid density data as well as binary VLE data are considered in the regression. Ramírez-Vélez et al.¹²¹ have shown that omission of either vapor pressure or saturated liquid density leads to poor predictions of the omitted property. This underlines the importance of including *both* pure-component vapor pressure and liquid density data in the regression. The pure-component pseudoexperimental vapor pressure and liquid density data used were taken from correlations given in the 2020 version of the DIPPR database.¹²² Instances in which the 2022 version of the DIPPR database¹²³ are used are stated explicitly. The

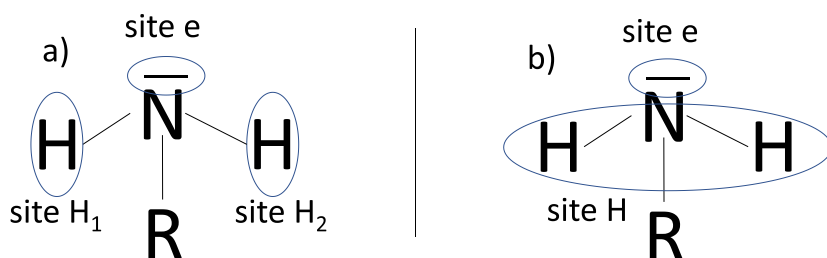


Figure 4. Illustration of a 3-site association scheme (a) and a 2-site scheme (b) for primary amines.

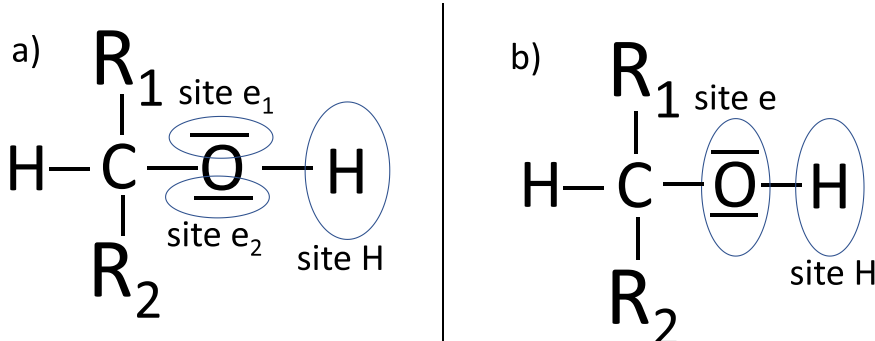


Figure 5. Illustration of a 3-site association scheme (a) and a 2-site scheme (b) for secondary alcohols.

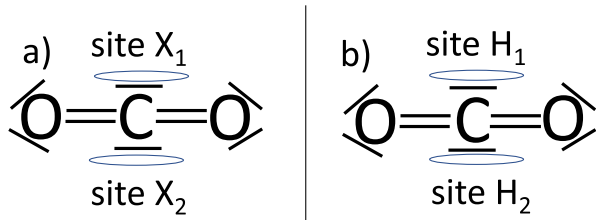


Figure 6. Illustration of a two cross-association site scheme ("2X") (a) and a scheme that only includes two electron acceptors (b) for CO_2 .

database provides a single correlation for each available property for each component.

Regarding the regressed binary VLE data, midlength species ought to be used where possible. These are likely to exhibit

traits of both the shorter and longer species. Therefore, they may yield improved accuracy for binary VLE predictions for species of a wide range of chain lengths. Moreover, the chosen systems should ideally exhibit azeotropes to aid the model in reproducing such challenging phase behavior. To fit the parameters to the data, a least-squares objective function was used in fitting the parameters.⁷¹ This was minimized with the Levenberg–Marquardt algorithm,^{124,125} unless explicitly stated otherwise. **Tables 2** and **3** provide details regarding the parameter fitting procedure.

It is worth noting that the s-SAFT- γ Mie model parameters are geared toward providing accurate descriptions of VLE, as opposed to liquid–liquid equilibria (LLE). The model is developed primarily for use in designing chemical absorption carbon capture processes, which rely heavily on accurate descriptions of VLE. Accordingly, pure component and binary

Table 2. Parameter Fitting Procedure Details the Systems Considered in This Work^a

species considered	primary amines	secondary alcohols	alkanolamines
functional groups present	CH_2NH_2 (NH_2), CH_3 , CH_2 Pure-Component Properties ^b	CHOH , CH_3 , CH_2 2-propanol to 2-nonanol	CH_2NH_2 (NH_2), CH_2OH (OH), CH_2 monoethanolamine
species included	ethylamine to decylamine	2-propanol to 2-nonanol	1
regression weight for pure-component properties	1	1	1
vapor pressure data points per component	30	30	30
saturated liquid density data points per component	30	30	30
Binary Mixture Data			
binary mixture data included	n -heptane/butylamine ¹²⁶	n -heptane/2-pentanol ¹²⁷	N/A
binary mixture data type	isothermal VLE (348.13 K)	isothermal VLE (348.15 K)	N/A
regression weight	7.5	18	N/A
number of data points	15	25	N/A
site schemes considered	CH_2NH_2 (NH_2): 2-site (1 e-1 H) or 3-site (1 e-2 H)	CHOH : 2-site (1 e-1 H) or 3-site (2 e-1 H)	CH_2OH (OH): 2-site (1 e-1 H) or 3-site (2 e-1 H)

^aAll pure-component data were regressed in ranges of $0.5T_c$ – $0.9T_c$. ^bPseudoexperimental data taken from the DIPPR database.¹²²

Table 3. Parameter Fitting Procedure Details for Systems Considered in This Work (Continued)

species considered	<i>n</i> -alkanes/CO ₂	primary alcohols/CO ₂	secondary alcohols/CO ₂
functional groups present	CO ₂ , CH ₃ , CH ₂	CH ₂ OH (OH), CO ₂ , CH ₃ , CH ₂	CHOH, CO ₂ , CH ₃ , CH ₂
site schemes considered	N/A	CH ₂ OH (OH): 2-site (1 e-1 H) or 3-site (2 e-1 H) CO ₂ : 2 H or 2 bipolar sites ("2 X")	CHOH: 2-site (1 e-1 H) or 3-site (2 e-1 H) CO ₂ : 2 H or 2 X
		Binary Mixture Data	
binary mixture data included	a) <i>n</i> -butane/CO ₂ ¹²⁸ b) <i>n</i> -hexane/CO ₂ ¹²⁹	ethanol/CO ₂ ¹³⁰	2-propanol/CO ₂ ¹³¹
binary mixture data type	a) isothermal VLE (250.00 K) b) isothermal VLE (298.15 K)	isothermal VLE (291.15 K)	isothermal VLE (293.25 K)
number of data points	a) 20 b) 10	10	12

mixture VLE data are used consistently in parametrizing the model.

3. RESULTS AND DISCUSSION

The s-SAFT- γ Mie size and shape parameters obtained for all functional groups with both the 2-site and 3-site schemes are given in Table 4, while the dispersion and repulsive exponent values are given in Tables 5 and 6. Tables 7 and 8 show the association parameters.

Table 4. s-SAFT- γ Mie Shape and Size Parameters

group <i>k</i>	<i>v</i> _{<i>k</i>} [*]	<i>S</i> _{<i>k</i>}	$\sigma_{kk}/\text{\AA}$	group size (<i>v</i> _{<i>k</i>} [*] <i>S</i> _{<i>k</i>} σ_{kk})
2-Site				
CH ₂ OH ^a	2	0.312	4.220	2.631
3-Site				
CH ₂ OH ^a	2	0.427	3.789	3.232
2-site				
OH	1	0.299	4.173	1.246
3-site				
OH	1	0.529	3.491	1.849
2-site				
CH ₂ NH ₂	2	0.472	3.834	3.616
3-site				
CH ₂ NH ₂	2	0.466	3.857	3.597
2-site				
NH ₂	1	0.631	3.570	2.254
3-site				
NH ₂	1	0.635	3.568	2.265
2-Site				
CHOH	2	0.250	4.130	2.066
3-Site				
CHOH	2	0.215	4.437	1.909
Not Self-Associating				
CO ₂ ^b	2	0.847	3.050	5.165

^aParameters of Schulze-Hulbe et al.⁷¹ ^bSAFT- γ Mie parameters of Papaioannou et al.⁹⁵

3.1. Primary Amines. **3.1.1. Physical Significance of Primary Amine Parameters.** The CH₂NH₂ group's size given in Table 4 (3.6 Å for both the 2-site and 3-site schemes) is somewhat larger than that of the CH₂OH group (2.6 Å for the 2-site scheme, and 3.2 Å for the 3-site scheme).⁷¹ The same trend can be inferred upon comparison of the OH and NH₂ groups. However, given the presence of an additional hydrogen relative to the primary alcohol group, a larger amine group can be expected. Furthermore, the CH₂NH₂ association energies

(1022 K (2-site scheme) and 911 K (3-site scheme)) are lower than the CH₂OH association energies (2990 K (2-site scheme) and 2594 K (3-site scheme)). This also holds for the smaller groups (NH₂ and OH, respectively), for both s-SAFT- γ Mie and SAFT- γ Mie.⁶⁶ Given the weaker electric dipole of nitrogen (3.07)¹³² relative to oxygen (3.50),¹³² weaker association is expected.

Moreover, the primary amine dispersion energies for the CH₂NH₂ group approximately lie within the range of ca. 350–460 K, while those for the NH₂ group lie within the range of ca. 350–600 K. These ranges are comparable with the approximate dispersion energy ranges of the CH₂OH (320–400 K) and OH (350–610 K) groups, respectively. Given that both families are constituted by linear carbon chains ending in an associating functional group, this broad agreement is also to be expected. Overall, these trends and consistencies suggest that the s-SAFT- γ Mie primary amine parameters are physically meaningful, echoing conclusions for the primary alcohol parameters.⁷¹

3.1.2. Primary Amine Vapor Pressure and Saturated Liquid Density. The systems discussed in this work are stepping stones in parametrizing the model for ternary alkanolamine/organic cosolvent/CO₂ mixtures. Therefore, less emphasis is placed on investigating the model performance for primary amines, secondary alcohols, or CO₂-containing binary mixtures. Previous work^{70,71} provided more in-depth investigations in this regard, as it served to explore s-SAFT- γ Mie's capabilities. Accordingly, pure-component property discussions will be limited to vapor pressure and saturated liquid density. Furthermore, binary mixture property discussions will be extended to VLE and excess enthalpy. The latter is included as it is a useful property in developing thermodynamic theories of mixtures,¹³³ particularly for organic species.¹³⁴

Table 9 provides the %AAD values for vapor pressure and saturated liquid density data of ethylamine to decylamine obtained with both the 2-site and 3-site s-SAFT- γ Mie parameter sets.

Percentage average absolute deviation (%AAD) quantifies a model's ability to reproduce experimental data. This is defined in eq 2.

$$\%AAD = \frac{100}{n_M} \sum_{i=1}^{n_M} \left| \frac{M_i^{\exp} - M_i^{\text{calc}}}{M_i^{\exp}} \right| \quad (2)$$

Table 5. s-SAFT- γ Mie Dispersion Energies and Repulsive Exponents

group <i>k</i>	group <i>l</i>	$(\epsilon_{kl}/k_B)/K$	λ_{kl}^r	λ_{kl}^a
CH_2OH^a	2-Site			
	CH_2OH^a	406.713	10.258	6
	CH_3	328.174	CR ^b	CR
	CH_2	339.612	CR	CR
	3-Site			
	CH_2OH^a	342.429	10.718	6
CH_2OH^a	CH_3	317.906	CR	CR
	CH_2	323.414	CR	CR
	2-Site			
	OH	608.665	8.605	6
	CH_3	320.321	CR	CR
	CH_2	353.164	CR	CR
OH	3-Site			
	OH	500.791	13.946	6
	CH_3	341.647	CR	CR
	CH_2	360.578	CR	CR
	2-Site			
	CH_2NH_2	463.855	18.620	6
CH_2NH_2	CH_3	351.842	CR	CR
	CH_2	372.172	CR	CR
	3-Site			
	CH_2NH_2	460.332	18.761	6
	CH_3	353.315	CR	CR
	CH_2	373.429	CR	CR
NH_2	2-Site			
	NH_2	584.185	22.496	6
	CH_3	350.575	CR	CR
	CH_2	390.334	CR	CR
	3-Site			
	NH_2	559.356	21.823	6
NH_2	CH_3	348.494	CR	CR
	CH_2	387.186	CR	CR
	2-Site			
	CHOH	723.472	17.657	6
	CH_3	451.450	CR	CR
	CH_2	422.589	CR	CR
CHOH	3-Site			
	CHOH	773.418	20.316	6
	CH_3	481.556	CR	CR
	CH_2	459.925	CR	CR
	Non-self-associating			
	CO_2^c	207.890	26.408	5.055
CO_2	CH_3	183.694	13.534	CR
	CH_2	190.456	11.071	CR

^aParameters from Schulze-Hulbe et al.⁷¹ ^bCR: Combining rule used.^cParameters from Papaioannou et al.⁹⁵

where n_M denotes the number of data points of property M . M_i^{exp} and M_i^{calc} are the experimental and calculated values of data point *i* of property M , respectively.

Table 9 shows that s-SAFT- γ Mie provides an accurate description of primary amine vapor pressure: The average %AAD is 2.6% for both the 2-site and 3-site schemes. Given the large number of species fitted, this can be considered an “accurate” description. Further, the low experimental vapor pressures of longer, higher-boiling amines result in a smaller denominator in eq 2, thereby inflating the %AAD of these species.

Table 6. s-SAFT- γ Mie Dispersion Energies and Repulsive Exponents (Continued)

group <i>k</i>	group <i>l</i>	$(\epsilon_{kl}/k_B)/K$	λ_{kl}^r	λ_{kl}^a
CH_2OH	2-Site (CH ₂ OH)/3-Site (CH ₂ NH ₂)			
	CH_2OH	414.843	CR ^a	CR
	2-Site (OH)/3-Site (NH ₂)			
	OH	516.225	CR	CR
	2-Site (CH ₂ OH)/2-Site (CHOH)			
	CH_2OH	350.404	CR	CR
CH_2OH	2-Site (CH ₂ OH)/2H (CO ₂)			
	CH_2OH	268.916	CR	CR
	2-Site (CH ₂ OH)/2X (CO ₂)			
	CO_2	264.902	CR	CR
	2-Site (CH ₂ OH)/No Sites (CO ₂)			
	CO_2	297.149	CR	CR
OH	2-Site (OH)/2H (CO ₂)			
	OH	328.129	CR	CR
	2-Site (CHOH)/2H (CO ₂)			
	CHOH	378.919	CR	CR
	2-Site (CHOH)/2X (CO ₂)			
	CO_2	377.806	CR	CR
CH_2NH_2	2-Site (CHOH)/No Sites (CO ₂)			
	CHOH	379.400	CR	CR
	2-Site (CH ₂ NH ₂)/No Sites (CO ₂)			
	CH_2NH_2			
	2-Site (CH ₂ NH ₂)/3-Site (CH ₂ NH ₂)			
	CH_2NH_2			

^aCR: Combining rule used.

Also, the description of saturated liquid density is very good with an average %AAD of 0.9% for both schemes. The best vapor pressure descriptions are obtained for butylamine. This is unsurprising, given that butylamine/*n*-heptane VLE data were used in fitting the parameters. The corresponding s-SAFT- γ Mie correlations to vapor pressure and saturated liquid density are shown in Figures S1 and S2, respectively.

Table 9 also shows that both the 2-site and the 3-site schemes provide very similar results for the CH₂NH₂ and the NH₂ groups. This corresponds with the primary alcohol results.⁷¹

Table 7 shows that the 2-site CH₂NH₂ association parameters are larger than the 3-site parameters. This also applies to the NH₂ group association parameters. This observation can be explained as follows: The 3-site scheme presents more possibilities for bond formation. This likely compensates for the smaller association parameters obtained with the 3-site scheme, accounting for the similarities between the results obtained for both schemes.

Furthermore, Table 9 shows that the vapor pressure and saturated liquid density descriptions obtained with the CH₂NH₂ group and those obtained with the NH₂ group are very similar. Yet the NH₂ group’s dispersion energy (584 K (2-site scheme) and 559 K (3-site scheme)) is considerably larger than that of the CH₂NH₂ group (463 K (2-site scheme) and 460 K (3-site scheme)). Interestingly, the same trend holds for the primary alcohols: the OH group’s dispersion energy (609 K (2-site scheme) and 501 K (3-site scheme)) is noticeably larger than that of the CH₂OH group (407 K (2-site scheme) and 342 K (3-site scheme)). This could be attributed to the more polar nature of the smaller group relative to that of the more electrically neutral CH₂NH₂ (CH₂OH) group.

3.1.3. Primary Amine/n-Alkane VLE and Excess Enthalpy. Figures 7 and 8 show s-SAFT- γ Mie binary VLE predictions for the *n*-hexane/butylamine and *n*-hexane/hexylamine systems, respectively.

Table 7. s-SAFT- γ Mie Association Parameters (Like Interactions)

group <i>k</i>	group <i>l</i>	site type <i>a</i> on group <i>k</i> (number of occurrences)	site type <i>b</i> on group <i>l</i> (number of occurrences)	$(\varepsilon_{kl,ab}^{HB}/k_B)/K$	$\kappa_{kl,ab}^{HB}/\text{\AA}^3$
2-Site					
CH ₂ OH ^a	CH ₂ OH ^a	e (1)	H (1)	2989.688	19.152
3-Site					
CH ₂ OH ^a	CH ₂ OH ^a	e (2)	H (1)	2594.053	17.271
2-Site					
OH	OH	e (1)	H (1)	2991.754	19.533
3-Site					
OH	OH	e (2)	H (1)	2502.904	22.086
2-Site					
CH ₂ NH ₂	CH ₂ NH ₂	e (1)	H (1)	1022.262	90.073
3-Site					
CH ₂ NH ₂	CH ₂ NH ₂	e (1)	H (2)	911.097	71.676
2-Site					
NH ₂	NH ₂	e (1)	H (1)	1030.371	105.041
3-Site					
NH ₂	NH ₂	e (1)	H (2)	932.059	76.448
2-Site					
CHOH	CHOH	e (1)	H (1)	2614.107	16.810
3-Site					
CHOH	CHOH	e (2)	H (1)	2365.533	14.149

^aParameters from Schulze-Hulbe et al.⁷¹

Table 8. s-SAFT- γ Mie Association Parameters (Unlike Interactions)

group <i>k</i>	group <i>l</i>	site type <i>a</i> on group <i>k</i> (number of occurrences)	site type <i>b</i> on group <i>l</i> (number of occurrences)	$(\varepsilon_{kl,ab}^{HB}/k_B)/K$	$\kappa_{kl,ab}^{HB}/\text{\AA}^3$
2-Site (CH ₂ OH)/3-Site (CH ₂ NH ₂)					
CH ₂ OH	CH ₂ NH ₂	H (1)	e (1)	2687.212	6.516
e (1)					
H (2)					
2-Site (OH)/3-Site (NH ₂)					
OH	NH ₂	H (1)	e (1)	2669.969	7.342
e (1)					
H (2)					
2-Site (CH ₂ OH)/2-Site (CHOH)					
CH ₂ OH	CHOH	H (1)	e (1)	1730.620	174.701
e (1)					
H (1)					
2-Site (CH ₂ OH)/2H (CO ₂)					
CH ₂ OH	CO ₂	e (1)	H (2)	1825.516	55.683
2-Site (CH ₂ OH)/2X (CO ₂)					
CH ₂ OH	CO ₂	H (1)	X (2)	1236.274	8.746
e (1)					
X (2)					
2-Site (OH)/2H (CO ₂)					
OH	CO ₂	e (1)	H (2)	1681.805	33.641
2-Site (CHOH)/2H (CO ₂)					
CHOH	CO ₂	e (1)	H (2)	894.905	3.095
2-Site (CHOH)/2X (CO ₂)					
CHOH	CO ₂	H (1)	X (2)	939.920	4.714
e (1)					
X (2)					

s-SAFT- γ Mie provides good predictions of the azeotropic *n*-hexane/butylamine system. The description of the *n*-hexane/hexylamine system is even better, although the hexylamine vapor pressure %AAD was 2.7% for the CH₂NH₂ group and 2.9% for the NH₂ group.

Additionally, Figure 8 shows that the bubble-point curve is greatly overestimated when primary amine/*n*-alkane VLE data are omitted from the regression. The parameters obtained without regressing the model to binary VLE are labeled “pure only” and are given in Tables S1–S3. This supports the notion that mixture data are instrumental in determining model parameters for associating groups. Furthermore, Figures 9 and

10 show the excess enthalpies of mixing (H^E) for the *n*-hexane/propylamine and *n*-hexane/decylamine systems, respectively.

s-SAFT- γ Mie provides accurate predictions of the excess *n*-hexane/propylamine enthalpy, although it underestimates the excess enthalpy of the *n*-hexane/decylamine system. Positive excess enthalpies ($H^E > 0$, endothermic mixing) indicate that breaking bonds between like molecules is the most significant energetic process during mixing.¹³⁹ Accordingly, underestimating positive excess enthalpies could indicate that the model underestimates the strength of pure-component intermolecular interactions for larger primary amines. This is supported by isobaric heat capacity predictions shown in Figure S3. Figure S3 shows that the model consistently underestimates the

Table 9. %AAD of Saturated Vapor Pressure (P^{sat}) and Saturated Liquid Density (ρ_{liq}^{sat}) Descriptions of Primary Amines Obtained with s-SAFT- γ Mie (Correlated Data)^a

	temperature range (K)	number of data points	P^{sat} %AAD				ρ_{liq}^{sat} %AAD			
			CH ₂ NH ₂		NH ₂		CH ₂ NH ₂		NH ₂	
			2-site	3-site	2-site	3-site	2-site	3-site	2-site	3-site
ethylamine	228–411	30	0.90	0.82	1.36	1.37	1.98	2.07	2.06	2.14
propylamine	248–447	30	1.82	1.77	2.11	2.07	0.46	0.49	0.51	0.54
butylamine	266–479	30	0.78	0.80	0.83	0.82	0.55	0.54	0.58	0.57
pentylamine	278–500	30	3.27	3.25	3.53	3.51	0.22	0.23	0.25	0.25
hexylamine	292–526	30	2.70	2.70	2.87	2.87	0.76	0.77	0.81	0.82
heptylamine	304–546	30	3.40	3.38	3.49	3.47	0.82	0.85	0.88	0.90
octylamine	314–564	30	3.28	3.27	3.46	3.44	0.37	0.41	0.44	0.47
nonylamine	324–583	30	4.22	4.21	4.45	4.43	0.69	0.73	0.77	0.79
decylamine	332–597	30	2.83	2.83	2.79	2.78	1.91	1.94	1.98	2.01
average			2.58	2.56	2.76	2.75	0.86	0.89	0.92	0.94

^aPseudoexperimental data taken from the DIPPR database.¹²²

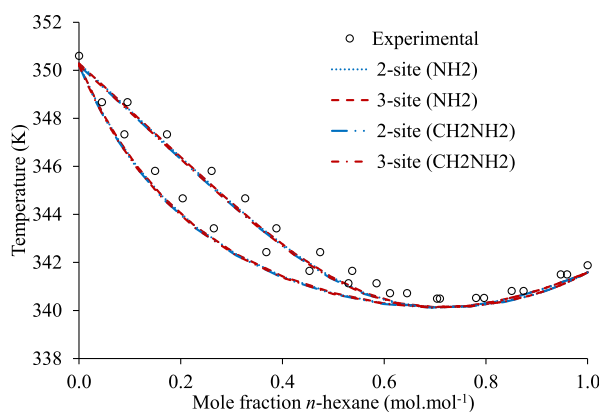


Figure 7. Isobaric binary VLE predictions for the *n*-hexane/butylamine system are shown at 1.01 bar. Experimental data taken from Dominguez et al.¹³⁵ Pure-component boiling points taken from the DIPPR database.¹²²

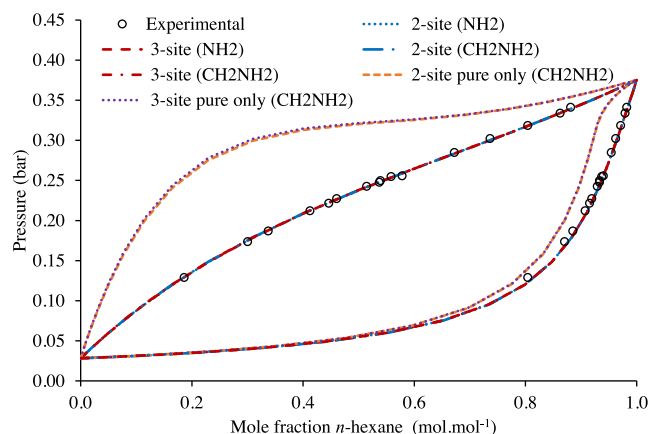


Figure 8. Isothermal binary VLE predictions of the *n*-hexane/hexylamine system at 313.1 K. Experimental data taken from Kern et al.¹³⁶

isobaric heat capacity of larger primary amines. This indicates that the model underestimates the energy required to raise the temperature of pure components, further suggesting that the strength of intermolecular interactions is undervalued in longer primary amines. Discussions of excess enthalpy should be viewed in context of the fact that describing excess enthalpy

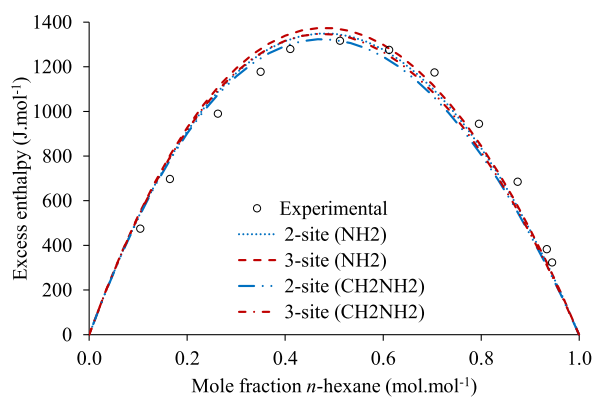


Figure 9. Excess enthalpy for the *n*-hexane/propylamine system at 303.1 K and 1.01 bar. Data taken from Velasco et al.¹³⁷

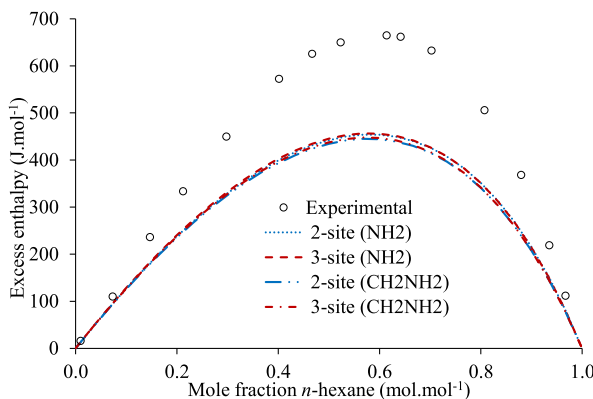


Figure 10. Excess enthalpy for the *n*-hexane/decylamine system at 313.2 K and 1.00 bar. Data taken from Fernandez et al.¹³⁸

challenging, given that subtle phenomena¹⁴⁰ and molecular details¹⁴¹ must be reproduced to describe it accurately. Accordingly, even a qualitatively accurate description of excess enthalpy can be deemed satisfactory and is common in this inherently predictive group-contribution modeling approach.

Although the above discussion indicates that the model provides poorer descriptions of excess enthalpy and isobaric heat capacity of longer amines, this does not necessarily hold for binary mixture VLE descriptions: after all, the model provides highly accurate descriptions of *n*-hexane/hexylamine VLE. Additional data are needed to determine whether

mixtures of *n*-alkanes with even longer amines are similarly accurate.

Yet the parameters developed in this work will ultimately be used in modeling ternary component carbon capture systems. Therefore, the diminished performance of longer-chained amines is acceptable: The amines used in chemical absorption carbon capture applications tend to be shorter species. An example is monoethanolamine (MEA), which is widely studied, commonly used and readily available.¹⁴² It is considered the benchmark molecule for alkanolamine-based carbon capture,¹⁴³ and has a short backbone consisting only of two carbon atoms.

As for the pure-component properties, the primary amine/*n*-alkane VLE and excess enthalpy results obtained with the fine- and coarse-grained primary amine groups are very similar. Moreover, this also holds for the primary alcohols: Figures S4–S7 illustrate that the CH₂OH and OH groups also provide very similar descriptions of vapor pressure, saturated liquid density, as well as primary alcohol/*n*-alkane VLE. The higher dispersion energies of the fine-grained NH₂ and OH groups indicate that the polarity of these groups is accounted for in the dispersion term. Although polar forces are highly directional and act over long distances, and dispersion forces are isotropic and short-ranged,¹⁴⁴ these larger dispersion energies appear not to affect model performance. However, this similarity in performance between fine- and coarse-grained groups may not hold for complex cross-associating mixtures: Papaioannou et al.⁴⁹ as well as Chremos et al.⁷⁷ have found that using fine-grained groups yields poorer SAFT- γ SW descriptions of aqueous mixtures of primary alcohols and amines, respectively.

On the one hand, fine-grained groups may yield additional flexibility in modeling branched species, thereby enhancing the model's predictivity. Conversely, it is possible that they may yield poor descriptions of cross-associating solutions. Additional work is required to determine the performance of fine- and coarse-grained groups for cross-associating fluids. Accordingly, the use of the OH group will be investigated in primary alcohol/CO₂ systems further below.

3.2. Secondary Alcohols. **3.2.1. Physical Significance of Secondary Alcohol Parameters.** Table 4 shows that the secondary alcohol (CHOH) functional group is smaller than the primary alcohol (CH₂OH) group: The former has a size of 2.1 Å (2-site scheme) or 1.9 Å (3-site scheme), whereas the latter has a size of 2.6 Å (2-site scheme) or 3.2 Å (3-site scheme). A smaller CHOH group is expected, given that it has one less hydrogen atom than the CH₂OH group.

The hydroxyl groups of secondary alcohols are located more centrally on the alcohol molecule than on the primary alcohols. Therefore, steric hindrance may weaken association effects for secondary alcohols. This is supported by the literature: Wójcicka and Kalinowska¹⁴⁵ showed that 2-butanol in solution with *n*-heptane has a reduced ability to associate relative to the corresponding 1-butanol/*n*-hexane mixture. Moreover, Palombo et al.¹⁴⁶ have found that fewer hydroxyl groups form association bonds in 2-octanol than in 1-octanol. This was attributed to steric hindrance effects.¹⁴⁶ Moreover, Palombo et al.¹⁴⁷ have found that the hydrogen bond strength is slightly weaker in 2-octanol than in 1-octanol. For both the 2-site and 3-site schemes, the secondary alcohol association parameters are smaller than those of the primary alcohols. This suggests that the effect of steric hindrance is reflected in the s-SAFT- γ Mie association parameters.

In contrast, the CH₂/CHOH and CH₃/CHOH dispersion energies are roughly 100–150 K higher than the CH₂/CH₂OH and CH₃/CH₂OH dispersion energies for both site schemes. More strikingly, the CHOH dispersion energy is approximately 350–400 K higher than the CH₂OH dispersion energy. This could suggest that the secondary alcohols compensate for the reduction in association bonds with the increased dispersive interactions. Given the discussion presented above, the secondary alcohol parameters appear to be broadly physically meaningful.

3.2.2. Secondary Alcohol Vapor Pressure and Saturated Liquid Density. Table 10 provides the %AAD values of vapor pressure and saturated liquid density predictions for 2-propanol to 2-nonanol obtained with s-SAFT- γ Mie.

Table 10. %AAD of Vapor Pressure (P^{sat}) and Saturated Liquid Density (ρ_{liq}^{sat}) Descriptions for Secondary Alcohols Obtained with s-SAFT- γ Mie (Correlated Data)^a

	P^{sat}		ρ_{liq}^{sat}	
	2-site	3-site	2-site	3-site
2-propanol	4.14	4.41	2.37	2.35
2-butanol	2.45	2.98	1.17	1.24
2-pentanol	1.90	1.57	0.40	0.48
2-hexanol	2.78	2.73	0.52	0.61
2-heptanol	2.31	2.41	1.09	1.22
2-octanol	3.32	3.31	2.55	2.67
2-nonanol	3.13	3.03	1.08	1.20
average	2.86	2.92	1.31	1.39

^aPseudoexperimental data obtained from DIPPR database.¹²²

The best fit to vapor pressure data (and saturated liquid density data) was obtained for 2-pentanol. This is again unsurprising, given that 2-pentanol/*n*-heptane VLE data were used to fit the parameters. The corresponding s-SAFT- γ Mie vapor pressure and saturated liquid density predictions are shown graphically in Figures S8 and S9, respectively. Table 10 shows that, as for the primary alcohols and amines, both the 2-site and 3-site schemes yield very similar results.

Table 7 shows that the 2-site association parameters are larger than the 3-site parameters, which is again consistent with the primary alcohols and amines. Echoing the discussion in section 3.1.2, this could suggest that the stronger bonds of the 2-site scheme are balanced with more numerous but weaker bonds obtained with the 3-site scheme.

At this point, s-SAFT- γ Mie parameters for the primary alcohol (CH₂OH) and secondary alcohol (CHOH) functional groups have been developed. Therefore, it is worth assessing the transferability of these model parameters to species that include both groups. As glycerol consists of two CH₂OH groups and one CHOH group, it provides an ideal opportunity in this regard. In addition, use of glycerol in carbon capture processes has garnered some attention,^{148–153} rendering it a suitable test case. Figure 11 shows s-SAFT- γ Mie results obtained with parameters regressed to vapor pressure and saturated liquid density data. The two-site CH₂OH/2-site CHOH association scheme combination was used. Predictions made with combining rules are also shown.

Figure 11 shows that s-SAFT- γ Mie significantly underestimates glycerol's volatility when combining rules are used. Regressing vapor pressure data leads to much improved results (%AAD = 1.6%). Consequently, these poor results can be

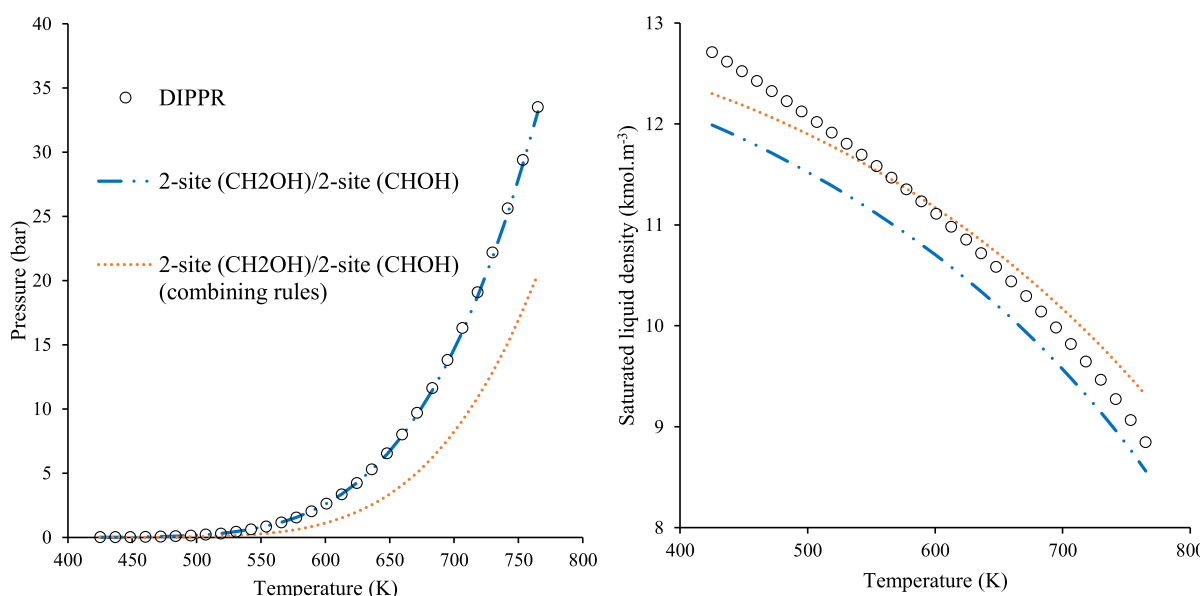


Figure 11. Vapor pressure (left) and saturated liquid density descriptions (right) for glycerol. “DIPPR” refers to pseudoexperimental data taken from the DIPPR database (2022 version).¹²²

attributed to combining rules and not underlying model performance. However, the saturated liquid density fit is mediocre for the regressed parameter set (%AAD = 4.0%). Noting that glycerol is a strongly associating species, this result may be due to hydrogen bond cooperativity effects that SAFT models do not account for.¹⁵⁴ Moreover, the mediocre fit to density may also be explained by the model’s inability to account for intramolecular hydrogen bonding, given that molecular simulation indicates the presence of such bonds in pure glycerol.¹⁵⁵

3.2.3. Secondary Alcohol/n-Alkane VLE and Excess Enthalpy

Figure 12 shows binary VLE predictions for the *n*-

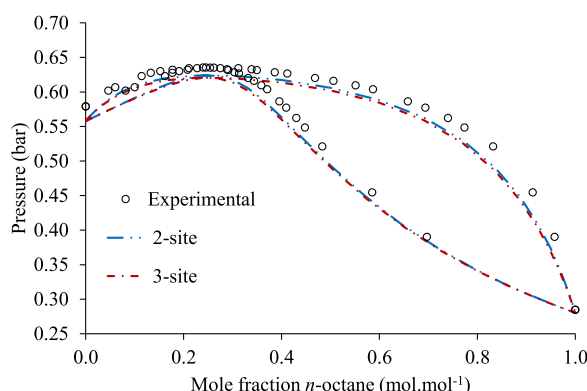


Figure 12. Isothermal binary VLE predictions for the *n*-octane/2-butanol system at 358.2 K. Experimental data taken from Hiaki et al.¹⁵⁶

octane/2-butanol system. The size asymmetry of the system components as well as the presence of azeotropes render the VLE of this system challenging to reproduce. However, s-SAFT- γ Mie provides accurate VLE predictions. Additionally, robust predictions of the similar *n*-octane/2-propanol VLE system are shown in **Figure S10**. The model’s good performance can partly be attributed to the inclusion of azeotropic 2-pentanol/*n*-heptane VLE data in the regression.

Moreover, **Figures 13 and 14** show excess enthalpy predictions for the *n*-nonane/2-hexanol and *n*-hexane/2-butanol systems.

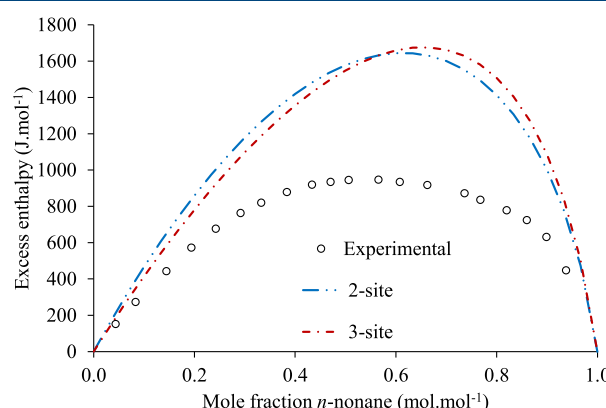


Figure 13. Excess enthalpy for the *n*-nonane/2-hexanol system at 298.2 K and 1.01 bar. Experimental data taken from Ortega.¹⁵⁷

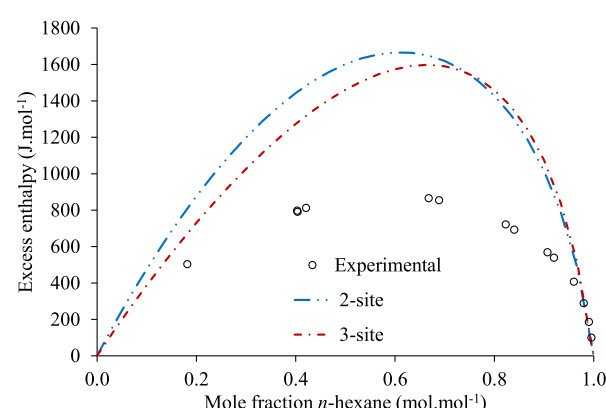


Figure 14. Excess enthalpy for the *n*-hexane/2-butanol system at 298.1 K and 1 bar. Experimental data taken from Brown et al.¹⁵⁸

Figures 13 and 14 show that s-SAFT- γ Mie tends to overestimate the excess enthalpies of the 2-alcohol/*n*-alkane systems. Similar findings were made for the primary alcohol/*n*-alkane excess enthalpies.⁷¹ As discussed in section 3.1.3, positive excess enthalpies indicate that breaking bonds between like molecules dominates the mixing process. Such an overestimation of the strength of such interactions may indicate that s-SAFT- γ Mie overvalues the strength of such interactions between secondary alcohols. Particularly, given the notably large values of the secondary alcohol dispersion energies (see Table 5), it is possible that dispersion interactions in secondary alcohols are overestimated.

3.2.4. Moving Beyond 2-Alcohols. Thus far, the discussion of secondary alcohols has been limited to 2-alcohols. It is stressed that higher secondary alcohols (i.e., 3- and 4-alcohols) were not included in the regression. Solely using species with the same hydroxyl group branch position (i.e., 2-alcohols) in the parametrization is consistent with previous work on branched alkanes.⁷⁰ Further, this predictive approach facilitates the assessment of how well model parameters can be transferred to higher secondary alcohols. Figure 15 depicts

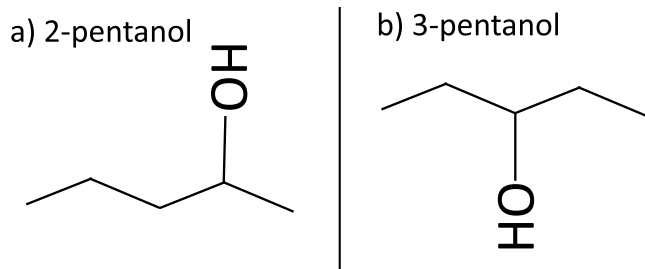


Figure 15. Illustration of secondary alcohol isomers 2-pentanol (a) and 3-pentanol (b).

the difference between the secondary alcohol isomers 2-pentanol and 3-pentanol, with Table 11 comparing their boiling points and critical points, as well as those of several other secondary alcohol isomers.

Table 11 clearly indicates that, for each chain length, the boiling point and critical point decrease as the hydroxyl group shifts toward the center of the molecule. This illustrates that 3-alcohols are more volatile than 2-alcohols, and 4-alcohols are more volatile than both 2- and 3-alcohols.

The blue dashed and dotted curves in Figure 16 show the s-SAFT- γ Mie vapor pressure descriptions for secondary alcohol isomers of pentanol, hexanol, and heptanol. Results obtained with the 3-site scheme are given in Figure S11.

Figure 16 illustrates that, although the vapor pressures of the secondary alcohol isomers differ, the s-SAFT- γ Mie descriptions of all the isomers for a given chain length (the blue dash-dotted curves) are near-identical. Although the model's chain term (the formulation of A^{chain} in eq 1) distinguishes between these isomers, the contribution of the chain term to the overall residual Helmholtz free energy is very small. This is shown in

Figure 17, which provides the relative contribution of each Helmholtz free energy term for liquid 2-pentanol and 3-pentanol at 293 K and 0.1095 m³.kmol⁻¹.

Therefore, the differences in the chain term between 2-pentanol and 3-pentanol are insufficient for distinguishing the thermodynamic properties of these associating isomers. Accordingly, further model modification is required to account for subtle volatility differences in secondary alcohols.

As discussed in section 3.2.1, steric hindrance effects appear to weaken the association in secondary alcohols. These effects may well differ between 2-alcohols, 3-alcohols, and 4-alcohols. Therefore, it is worth investigating whether adaptations to the association term provide improved model results for higher secondary alcohols (3- and 4-alcohols). It is stressed that an appropriate modification to the association term would need to yield improved predictions of secondary alcohol properties, beyond merely providing improved correlations to fitted data.

Key to the association term is the association strength parameter $\Delta_{ij,kl,ab}$, which characterizes the association bond between a site of type *a* on group *k* of molecule *i* and a site of type *b* of group *l* of molecule *j*. It is a function of the association energy and volume, as defined in eq 3 below.⁶⁶

$$\Delta_{ij,kl,ab} = \left(\exp\left(\frac{e_{kl,ab}^{\text{HB}}}{k_B T}\right) - 1 \right) \kappa_{kl,ab} I_{ij,kl,ab} \quad (3)$$

where $I_{ij,kl,ab}$ is a polynomial temperature-density correlation of the association integral for Lennard-Jones segments, as discussed by Haslam et al.⁶⁶

A simple modification to $\Delta_{ij,kl,ab}$ is proposed, which accounts for the effect of hydroxyl group location. This is shown in eq 4 below.

$$(\Delta_{ij,kl,ab})_{\text{mod}} = \Delta_{ij,kl,ab}(1 - AP) \quad (4)$$

where *A* is an empirical factor regressed to experimental data and *P* is the position of the hydroxyl group branch on the carbon chain. For instance, *P* = 3 for a 3-alcohol. For 2-alcohols, *A* = 0, so that the association strength assumes its original value. The subscript "mod" in eq 4 indicates that the association strength has been modified.

The existing 2-site and 3-site secondary alcohol parameters are used in fitting the association modification parameter *A* to vapor pressure and saturated liquid density data. Details regarding the fitting procedure are listed in Table 12.

Reduced temperature intervals are used for the vapor pressure data for 3-heptanol (0.5T_c–0.8T_c) and 4-heptanol (0.5T_c–0.75T_c). At temperatures above these ranges, the vapor pressure data for these components exhibit reduced volatility relative to 2-heptanol, rendering their quality questionable. Moreover, the pseudoexperimental density data are taken from correlations fitted to experimental data which do not extend above approximately 0.7T_c. The temperature intervals for the saturated liquid density are chosen accordingly to prevent extrapolating the correlations to temperatures where there are no measured data (i.e., *T* < 0.7T_c).

Table 11. Boiling Points and Critical Points for Several Secondary Alcohol Isomers

	2-pentanol	3-pentanol	2-hexanol	3-hexanol	2-heptanol	3-heptanol	4-heptanol
boiling point (K)	392.2	388.5	412.4	406.2	432.9	429.2	427.8
critical point (K)	561	559.6	585.3	582.4	608.3	605.4	602.6
reference				DIPPR ¹²²			NIST ¹⁵⁹

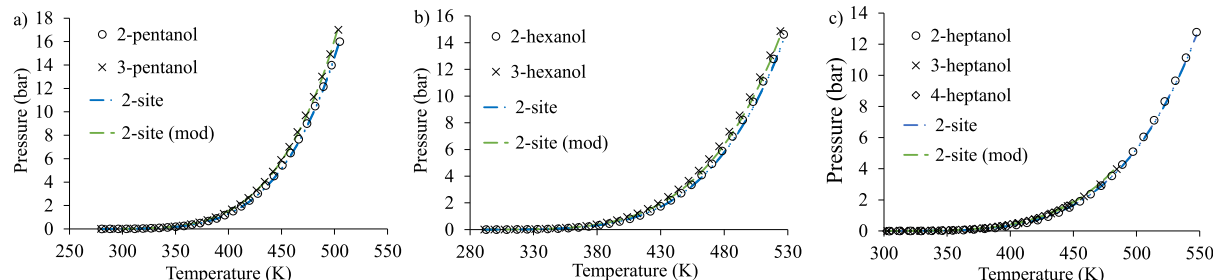


Figure 16. Saturated vapor pressures of secondary alcohol isomers of pentanol (a), hexanol (b), and heptanol (c) obtained with s-SAFT- γ Mie. Chain length increases from left to right. The 2- and 3-alcohol data were obtained from the DIPPR database,¹²² while 4-heptanol data were taken from NIST.¹⁵⁹

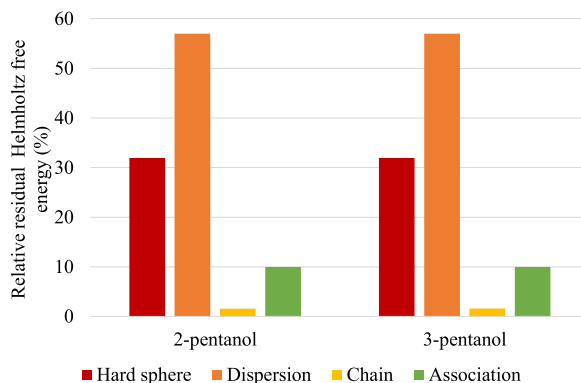


Figure 17. Contributions of the s-SAFT- γ Mie Helmholtz energy terms to the relative residual Helmholtz free energy (A^{res}) for 2-pentanol and 3-pentanol at 293.2 K and $0.1095 \text{ m}^3 \cdot \text{kmol}^{-1}$. 3-Site scheme parameters were used.

For the 2-site scheme, $A = 0.113$, whereas $A = 0.103$ for the 3-site scheme. Figure 18 shows that the model modification only marginally decreases the Helmholtz free energy contribution of the association term.

Despite these minor effects on the Helmholtz free energy, Figure 16 shows that the modified association term (indicated with the green dashed line) generally provides significantly improved descriptions of 3-alcohol (and 4-alcohol) vapor pressures, which are distinct from the 2-alcohol descriptions. The improvement for 3-pentanol is particularly noteworthy: The %AAD improves from ca. 17% to ca. 3%, for both schemes, although the A parameter was not regressed to any 3-pentanol data. Unfortunately, a lack of reliable data for 4-alcohols limits the investigation of pure-component-properties of secondary alcohols. Nonetheless, Table 13 shows that the modification significantly improves the description of the vapor pressure of 4-undecanol and 4-tridecanol for both association schemes at the cost of only slight decreases in accuracy for the saturated liquid density (ca. 0.5%).

This investigation is further extended to the 3-alcohol/*n*-alkane VLE. Figure 19 shows s-SAFT- γ Mie binary VLE predictions for the *n*-heptane/3-pentanol system. SAFT- γ Mie

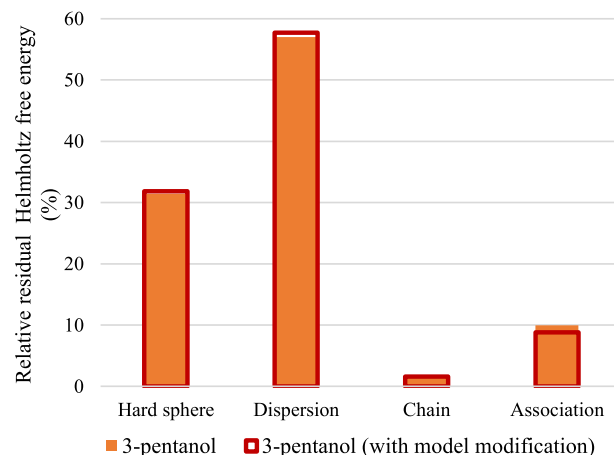


Figure 18. Contributions of the s-SAFT- γ Mie Helmholtz free energy terms to the relative residual Helmholtz energy (A^{res}) for 3-pentanol at 293.2 K and $0.1095 \text{ m}^3 \cdot \text{kmol}^{-1}$. The 3-site scheme parameters are used.

results are included for comparison. Results for this system obtained with the 3-site scheme parameters are shown in Figure S12.

The model modification provides a better estimate of the 3-pentanol boiling point than both the unmodified model as well as SAFT- γ Mie (with parameters taken from Haslam et al.).⁶⁶ It also provides greatly improved estimates of the shape of the phase envelopes relative to the unmodified model. More reliable property data for 4- and 5-alcohols are required to further assess the model modification. Nonetheless, these results indicate that it sensibly accounts for the change in phase equilibria effected by changing the hydroxyl group position in secondary alcohols.

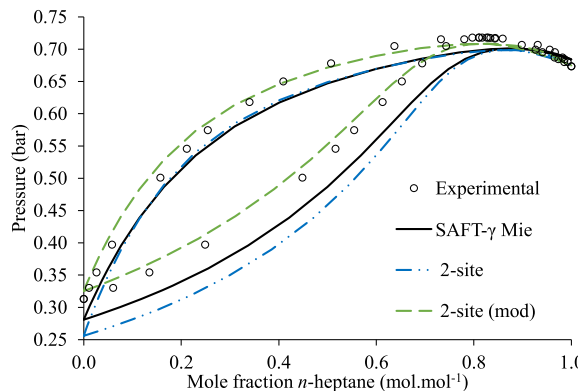
3.3. Alkanolamines. s-SAFT- γ Mie is further extended to linear alkanolamines. Noting the above-mentioned industrial relevance of MEA (section 3.1), the parameters are regressed to MEA vapor pressure and saturated liquid density data. This parametrization approach enables prediction of the properties of 3-amino-1-propanol and 6-amino-1-hexanol, thereby facil-

Table 12. Pseudo-Experimental Vapor Pressure (P^{sat}) and Saturated Liquid Density (ρ_{liq}^{sat}) Data Used in Fitting the A Parameter

component	P^{sat} data temperature range	number of P^{sat} data points	ρ_{liq}^{sat} data temperature range	number of ρ_{liq}^{sat} data points	data source
3-hexanol	$0.5T_c - 0.9T_c$	30	$0.5T_c - 0.7T_c$	15	DIPPR ¹²²
3-heptanol	$0.5T_c - 0.8T_c$	23	$0.5T_c - 0.7T_c$	15	DIPPR ¹²²
4-heptanol	$0.5T_c - 0.75T_c$	19	$0.5T_c - 0.7T_c$	12	NIST ¹⁵⁹

Table 13. %AAD of Saturated Vapor Pressure (P^{sat}) and Saturated Liquid Density (ρ_{liq}^{sat}) Predictions of Higher Secondary Alcohols Obtained with s-SAFT- γ Mie

component	P^{sat} %AAD				ρ_{liq}^{sat} %AAD				data source
	2-site	2-site (mod)	3-site	3-site (mod)	2-site	2-site (mod)	3-site	3-site (mod)	
4-undecanol	16.62	6.70	17.24	7.54	1.33	1.88	1.40	2.00	NIST ¹⁵⁹
4-tridecanol	6.69	4.96	7.06	4.21	2.16	2.66	2.23	2.76	NIST ¹⁵⁹

**Figure 19.** Isothermal binary VLE predictions for the *n*-heptane/3-pentanol system at 358.2 K. Experimental data taken from Linek and Wichterle.¹⁶⁰

tating a fair assessment of model capabilities. No alkanolamine/*n*-alkane binary VLE data are included in the parametrization, given the acute scarcity of such data. Use of VLE data for *nonassociating* *n*-alkanes with *associating* alkanolamine VLE data is a deliberate choice: Regressing alkanolamine parameters to data in which association plays a diminished role should aid the model in distinguishing between dispersive and associative interactions, providing more meaningful parameters with greater predictive capabilities. Although alkanolamine/primary alcohol data are available, they cannot aid the model in distinguishing between association and dispersion given that alkanolamines self-associate and cross-associate with primary alcohols. Accordingly, alkanolamine and primary alcohol data were not used as a surrogate for alkanolamine/*n*-alkane data. This parametrization choice is not without precedent: In their work on modeling ethers and esters with dipolar variants of PC-SAFT, Dominik et al.⁹⁷ restricted the mixture data in their parametrization to mixtures of ethers/esters with nonassociating and nonpolar fluids (i.e., alkanes). This was done to ensure that the fitting procedure yielded unique model parameters.⁹⁷

In regressing alkanolamine model parameters, both the primary amine and primary alcohol 2-site and 3-site association schemes were used. The parameters previously obtained for primary amines and primary alcohols were retained. Only the dispersion energies and association parameters between the CH₂NH₂ (NH₂) and CH₂OH (OH) parameters were regressed. Table 14 shows the %AADs for pure-component alkanolamine vapor pressure and saturated liquid density obtained with s-SAFT- γ Mie for the 2-site CH₂OH (OH)/3-site CH₂NH₂ (NH₂) combination.

Although the model provides good correlations for the vapor pressure of MEA, it yields poor predictions of the vapor pressures for 3-amino-1-propanol and 6-amino-1-hexanol. This is the case when both coarse-grained groups (CH₂OH and CH₂NH₂) and fine-grained groups (OH and NH₂) are used. These results suggest that the primary amine and primary alcohol parameters are not readily transferable across chemical

Table 14. %AAD of Alkanolamine Vapor Pressure (P^{sat}) and Saturated Liquid Density (ρ_{liq}^{sat}) Descriptions Obtained with s-SAFT- γ Mie^a

property type	species			
	monoethanolamine	3-amino-1-propanol	6-amino-1-hexanol	average
2-Site (CH ₂ OH)/3-Site (CH ₂ NH ₂)				
P^{sat}	0.33	34.26	32.99	22.53
ρ_{liq}^{sat}	2.22	3.04	N/A	2.63
2-Site (OH)/3-Site (NH ₂)				
P^{sat}	0.29	34.88	33.38	22.85
ρ_{liq}^{sat}	2.01	2.97	N/A	2.49
2-Site (CH ₂ OH)/3-Site (CH ₂ NH ₂) (Combining Rules)				
P^{sat}	3.85	34.81	36.31	24.99
ρ_{liq}^{sat}	2.09	3.16	N/A	2.63

^aPseudoexperimental data obtained from the DIPPR database (2022).¹²³ In each case, 30 temperatures in the interval 0.5T_c–0.9T_c were used.

families. Moreover, given that the model is only fitted to MEA data, the density fit (a %AAD of 2.2%) can be considered mediocre. Echoing the above discussion of s-SAFT- γ Mie results for glycerol, this may be due the model's inability to account for hydrogen bond cooperativity.¹⁵⁴

Very similar results to those obtained with the 2-site (CH₂OH)/3-site (CH₂NH₂) combination are obtained with the other site scheme combinations, as shown in Table S4. The corresponding parameter values for these site scheme combinations are given in Tables S2 and S3. Noting the similarity across the site scheme combinations, only the 2-site CH₂OH and 3-site CH₂NH₂ parameters will be carried forward in the development of the s-SAFT- γ Mie model parameters.

Further, Table 14 shows that the parameters obtained with combining rules are, on average, less accurate than the regressed parameters for the two-site (CH₂OH)/3-site (CH₂NH₂) combination. However, Table S4 shows that the converse holds for the 3-site (CH₂OH)/2-site (CH₂NH₂) parameters. The finding that a combining rule can provide better predictions than a regressed parameter set is further testament to the poor transferability of parameters across families. These results echo the work of Crespo et al.,¹⁶¹ who investigated the transferability of SAFT- γ Mie parameters for the ethylene oxide (EO) group across several chemical families. The EO group contains two CH₂ groups and an oxygen atom. These authors found that the model required refitting to accurately describe a given chemical family, or even for individual systems.¹⁶¹

3.4. CO₂-Containing Binary Mixtures. **3.4.1. *n*-Alkane/CO₂ Mixtures.** In the following, the s-SAFT- γ Mie EoS is extended to CO₂-containing binary mixtures. A necessary starting point for developing the model for these systems is obtaining the *n*-alkane/CO₂ parameters. Accordingly, the CH₂/CO₂ and CH₃/CO₂ dispersion energies and repulsive

exponents were regressed to *n*-butane/CO₂ VLE data.¹²⁸ Although this resulted in unrealistically low values of the CH₃/CO₂ dispersion energy, including *n*-hexane/CO₂ VLE data¹²⁹ remedied this issue. Moreover, regressing the CH₂/CO₂ and CH₃/CO₂ repulsive exponents enhanced the predictive capabilities of the model.

Figures 20 and 21 show s-SAFT- γ Mie VLE predictions for the systems ethane/CO₂ and *n*-pentane/CO₂. The parameter

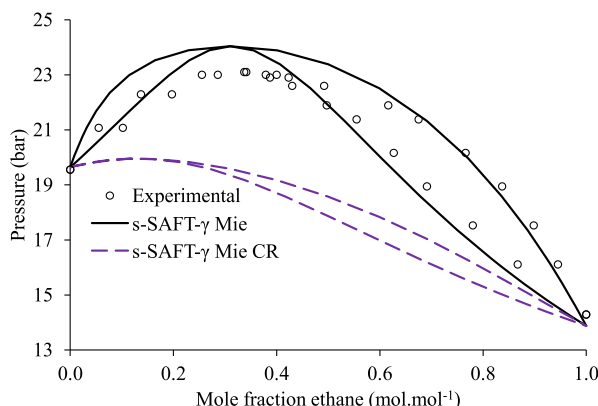


Figure 20. Isothermal ethane/CO₂ VLE at 253.0 K. Experimental data taken from Nagahama et al.¹⁶²

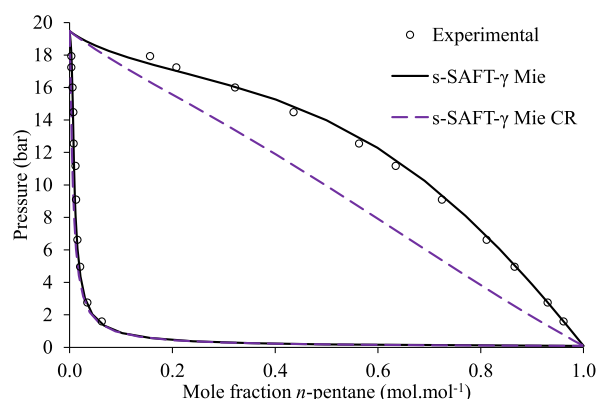


Figure 21. Isothermal *n*-pentane/CO₂ VLE at 252.7 K. Experimental data taken from Cheng et al.¹⁶³

sets labeled “CR” were obtained with a combining rule for the dispersion energy given in previous work.⁷¹

The figures show that use of the combining rule yields a poor estimate of the bubble-point curves of both systems and the dew point curve of the ethane/CO₂ system. This renders it ill-suited for use. Parameterizing the model with *n*-alkane/CO₂ VLE data, on the other hand, provides much more accurate results for both the ethane/CO₂ and the *n*-pentane/CO₂ systems. Doing so enables s-SAFT- γ Mie to predict the azeotrope for the ethane/CO₂ system fairly accurately, although it was not correlated to any azeotropic VLE data. These results suggest that s-SAFT- γ Mie provides a very good description of the *n*-alkane/CO₂ interactions. Therefore, these parameters are suitable for use as foundational building blocks for describing mixtures of other species with CO₂.

Excess enthalpies for CO₂-containing mixtures are not shown, as most of these data have been measured near or above the critical point of CO₂. SAFT-type EoSs are ill-suited for describing the critical region: Close to the critical point, density fluctuations occur, which are neglected by SAFT-type

EoSs.¹⁶⁴ Moreover, the aim of this work is to develop parameters for chemical absorption and carbon capture processes. These operate far from critical conditions (typically at atmospheric pressure and 100–120 °C).¹⁶⁵ Accordingly, the parameters used in this work are explicitly for use in the subcritical region.

3.4.2. Primary Alcohol/CO₂ Mixtures. s-SAFT- γ Mie is further extended to primary alcohol/CO₂ systems. In doing so, particular care must be taken in regressing parameters to primary alcohol/CO₂ binary mixture data: Some of these systems are classified as type III or type IV mixtures according to the classification of van Kreijenburg and Scott.¹⁶⁶ This means that, when approaching the critical point of CO₂, the mixture may reach critical behavior at temperatures and pressures below CO₂'s critical point. Therefore, it can be challenging to distinguish phase equilibria data sets in which the mixture is subcritical from those which reach a mixture critical point. The type III phase behavior exhibited by 1-hexanol/CO₂,^{167,168} as well as the type IV behavior of 1-pentanol/CO₂,^{167,169} are illustrated in the pressure–temperature plane in Figure 22a,b, respectively.

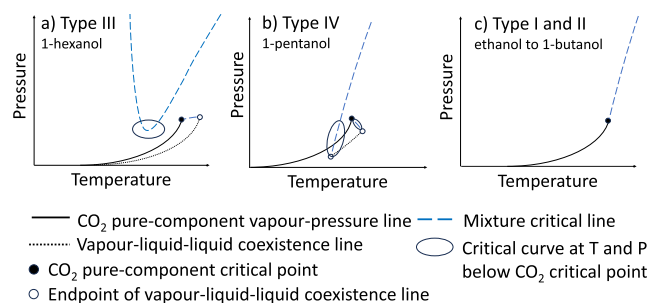


Figure 22. Key aspects of the van Kreijenburg and Scott¹⁶⁶ phase behavior types exhibited by binary mixtures of CO₂ with ethanol,¹⁷⁰ 1-propanol,¹⁷¹ 1-butanol,^{172,173} 1-pentanol,^{167,169} or 1-hexanol.^{167,168}

To prevent unwittingly regressing mixture critical points, it is sensible to consider solely the series of binary systems from ethanol/CO₂ to 1-butanol/CO₂ as candidates for the regression. These are type I or type II systems,^{170–173} which are also illustrated in Figure 22 c). For these systems, the critical lines do not fall to $T < T_{crit,CO_2}$ and $P < P_{crit,CO_2}$ in the vicinity of the CO₂ critical point. This means that the critical point can be used to distinguish binary VLE data that are subcritical from those that terminate in a mixture critical point.

Longer primary alcohols are not considered for inclusion in the regression. Given the length of these components, the phase behavior is likely to be dominated by the interactions between CO₂ and the alkyl backbone, rendering them ill-suited for parametrizing interactions between the CH₂OH and CO₂ groups.

s-SAFT- γ Mie showed a tendency to exhibit liquid–liquid phase splits when regressed to the 1-propanol/CO₂ and 1-butanol/CO₂ data. Lam et al.¹⁷⁴ have observed liquid–liquid phase splits for mixtures of CO₂ with 1-propanol and 1-butanol experimentally. However, they also report that VLLE only occurs well below the conditions at which s-SAFT- γ Mie determines phase splits (246 K and 15 bar for 1-propanol/CO₂ and 260 K and 23 bar for 1-butanol/CO₂, respectively). Therefore, the model is in error in predicting these phase splits.

Model predictions of liquid–liquid phase splits have been documented for SAFT- γ SW and SAFT- γ Mie modeling of the ethanol/CO₂ system,^{69,78} as well as for Peng–Robinson modeling of 1-propanol/CO₂ VLE.¹⁷¹ More generally, Polishuk et al.¹⁷⁵ have shown that liquid-phase immiscibility is commonly predicted in modeling critical loci for binary systems involving *n*-alkanes. s-SAFT- γ Mie predicted no additional liquid phase for the ethanol/CO₂ system. Therefore, this system was ultimately used in the parametrization.

Various parameter sets were used to determine how best to describe primary alcohol/CO₂ VLE: a 2-site CH₂OH group with either a 2H or 2X CO₂ association scheme, as well as a non-cross-associating parameter set. As discussed in section 3.1, the use of a fine-grained (OH) group was also assessed. Combinations involving a three-site CH₂OH association scheme are shown in Figures S13 and S14, with the corresponding parameters given in Tables S2 and S3. While the 2-site CH₂OH/2X CO₂ and 3-site CH₂OH/2X CO₂ combinations yielded very similar results, the 3-site CH₂OH/2H CO₂ combination provided worse correlations to the ethanol/CO₂ system, as it significantly overestimates the bubble-point curve. The overestimation of the bubble-point curve appears to bias this set toward higher vapor pressures. This yields an improved description of the phase equilibria of CO₂ with higher primary alcohols. For the 1-hexanol/CO₂ system (Figure S14), the 3-site CH₂OH/2H CO₂ combination is the only parameter set which predicts this system's liquid–liquid immiscibility at higher pressures, albeit inaccurately. Yet these improvements are likely due to the 3-site CH₂OH/2H CO₂ combination's inability to accurately correlate the ethanol/CO₂ data. Use of different regression algorithms did not yield significant improvements in fitting the parameters to these data.

Considering the above, the following discussion is limited to results obtained with the two-site CH₂OH (OH) scheme. Figure 23 shows the s-SAFT- γ Mie correlation to ethanol/CO₂ VLE data, whereas Figure 24 shows 1-hexanol/CO₂ VLE.

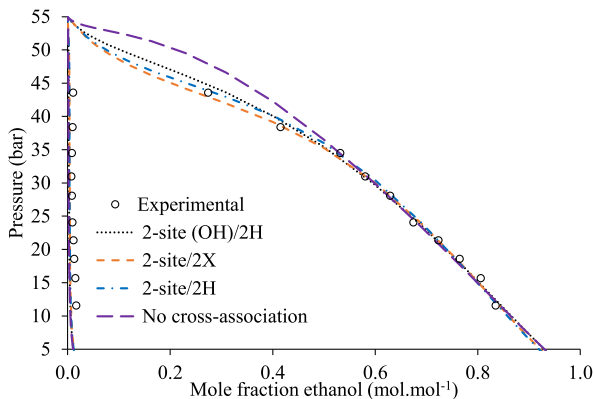


Figure 23. Isothermal ethanol/CO₂ VLE at 291.2 K. Experimental data taken from Chang et al.¹³⁰

Figure 23 shows that omitting cross-association leads to an overestimation of the bubble-point pressure at lower ethanol mole fractions, whereas incorporating it yields very accurate descriptions of the ethanol/CO₂ VLE data. However, predictions for the 1-hexanol/CO₂ bubble-point curve (Figure 24) are much worse. Results are somewhat improved by neglecting cross-association, although they remain poor.

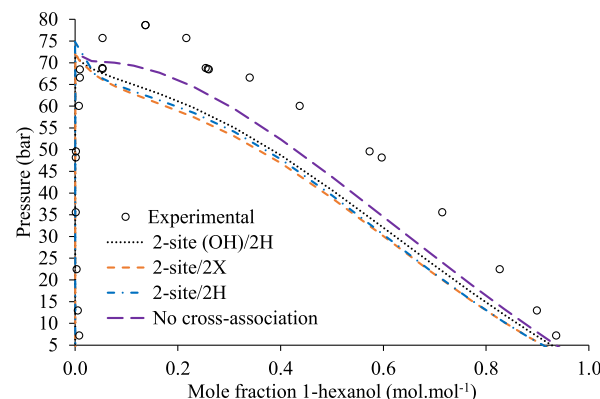


Figure 24. Isothermal 1-hexanol/CO₂ VLE at 303.2 K. Experimental data taken from Secuianu et al.¹⁶⁸

The overestimated bubble point pressures for ethanol/CO₂ VLE obtained with the “no cross-association” parameter set may well bias this parameter set toward higher bubble point pressures, as for the 3-site/2H association scheme combination. Accordingly, the improved 1-hexanol/CO₂ results obtained when neglecting cross-association are likely not the result of a fundamental improvement in the description of these systems but due to the “no cross-association” parameter set’s inability to correlate ethanol/CO₂ VLE. Moreover, as discussed in section 2.1, cross-association interactions do occur in these systems. Therefore, neglecting them is arguably a misrepresentation of primary alcohol/CO₂ interactions. Accordingly, the non-cross-associating sets will not be carried forward to further work.

Although the 2X scheme for CO₂ has more fitted parameters than the 2H scheme, both Figures 23 and 24 show that this does not translate to improved results. Additional association parameters are justifiable only if they enhance the model’s predictive capabilities. Accordingly, the 2H scheme for CO₂ is chosen over the 2X scheme for further development of the model.

Furthermore, the similar results obtained with the fine-grained (OH) and coarse-grained (CH₂OH) primary alcohol groups suggest that the use of fine-grained functional groups does not degrade the description of cross-associating mixtures, though that possibility was postulated in section 3.1. Accordingly, use of both the fine-grained and coarse-grained groups is carried forward in developing s-SAFT- γ Mie.

3.4.3. Secondary Alcohol/CO₂ Mixtures. The next step in developing the model is to parametrize secondary alcohol/CO₂ systems. In regressing model parameters for these systems, it was found that the Levenberg–Marquardt algorithm had difficulty in minimizing the objective function. This may be due to highly correlated model parameters, which yield an objective function that is highly insensitive to the regressed parameters. To circumvent this problem, the Simulated Annealing global optimization routine available in MATLAB was used. This algorithm searches the parameter space probabilistically, rendering it well-suited for a wide range of complex objective functions.

As for primary alcohol/CO₂ systems, the possibility of fitting near-critical data was precluded by ensuring that no type III or IV systems were considered in the regression. Indeed, the 2-butanol/CO₂ and 2-pentanol/CO₂ systems are type I or type II systems.^{176–178} Further, a literature survey by Sima et al.¹⁷⁹ suggests that 2-propanol/CO₂ appears to be either a type I or

type II system. Regressions with the 2-butanol/CO₂ VLE resulted in model predictions of liquid–liquid phase splits for that system. Given that this VLLE behavior was predicted above the experimental upper critical end point (VLLE limit) of 17.8 bar and 251 K,¹⁸⁰ it is certainly erroneous. 2-Propanol/CO₂ VLE¹³¹ were instead used in the regression. No phase splits were detected for the regressed 2-propanol/CO₂ system.

VLE predictions for the 2-propanol/CO₂ and 2-butanol/CO₂ systems are shown in Figures 25 and 26. The same

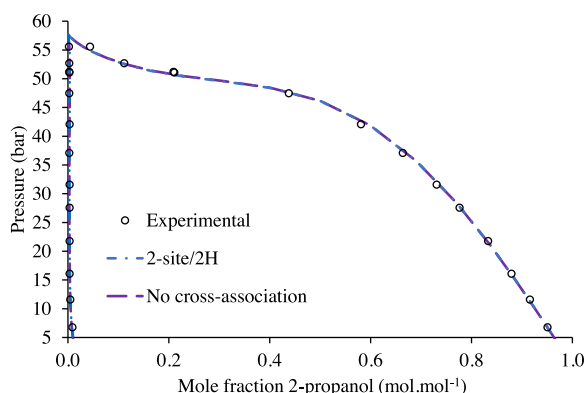


Figure 25. Isothermal 2-propanol/CO₂ VLE at 293.3 K. Experimental data taken from Secuiianu et al.¹³¹

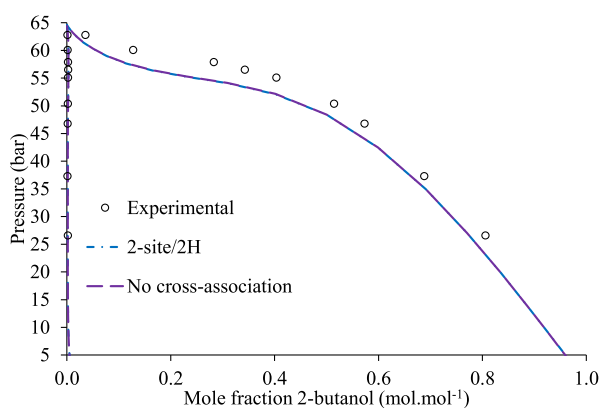


Figure 26. Isothermal 2-butanol/CO₂ VLE at 298.2 K. Experimental data taken from Secuiianu et al.¹⁷⁶

combinations of association schemes used for primary alcohols were also used for secondary alcohols. Only the 2-site CHOH/2H CO₂ combination results are shown, with all other schemes yielding similar results. Consistent with the primary alcohols, this parameter set is carried forward for further work. Results obtained with alternative parameter sets are shown in Figures S15 and S16, and the corresponding model parameters are given in Tables S2 and S3.

The width of the phase envelopes of both systems indicates that they are highly nonideal. The accurate description thereof is a testament to the noteworthy capabilities of s-SAFT- γ Mie, although the model underestimates the bubble-point pressures of the 2-butanol/CO₂ system.

In contrast to the primary alcohol/CO₂ mixtures, however, the “no cross-association” parameter set yields results that are nearly identical to those that account for cross-association. This suggests that cross-association may be less significant in secondary alcohols. This notion is supported by the higher dispersion energies (Table 6) and lower association parameters

(Table 8) for secondary alcohol/CO₂ interactions relative to primary alcohol/CO₂ interactions. This could be due to increased steric hindrance effects in secondary alcohols. Nonetheless, in keeping with the treatment of primary alcohol/CO₂ systems, cross-association will be accounted for in secondary alcohol/CO₂ systems.

4. CONCLUSIONS

In this work, the s-SAFT- γ Mie EoS was developed toward a description of nonaqueous alkanolamine-based carbon capture. This entailed extending the model to primary amines, secondary alcohols, alkanolamines, *n*-alkane/CO₂ mixtures, as well as primary alcohol/CO₂ and secondary alcohol/CO₂ mixtures. The model was found to provide accurate phase equilibria descriptions of primary amines and secondary alcohols as well as binary mixtures of primary amines or secondary alcohols with *n*-alkanes. s-SAFT- γ Mie was found to have poor predictive capabilities for linear alkanolamines, suggesting that the transferability of associating functional groups across chemical families is challenging for the model. It nonetheless provides robust descriptions of MEA, an alkanolamine of key importance in chemical absorption carbon capture.

s-SAFT- γ Mie was found to provide poor phase equilibria predictions for higher secondary alcohols (e.g., 3-alcohols and 4-alcohols), indicating that it fails to account for the change in intermolecular interaction with shifting hydroxyl group position along the carbon backbone. Descriptions of higher secondary alcohols, as well as their mixtures with *n*-alkanes, were much improved by applying an empirical modification to the association strength parameter ($\Delta_{ijkl,ab}$) to account for changes in associative interactions with changing hydroxyl group position.

Moreover, s-SAFT- γ Mie was found to provide accurate descriptions of *n*-alkane/CO₂ systems, although it had poor predictive capabilities for highly nonideal mixtures of CO₂ with primary and secondary alcohols. Nonetheless, the model provided accurate descriptions in the low-pressure region relevant for chemical absorption carbon capture.

In developing the parameters thus discussed, the use of fine-grained functional groups (OH and NH₂) versus more coarse-grained groups (CH₂OH and CH₂NH₂) was investigated. Fine- and coarse-grained groups were found to yield equivalent results. Both group types are carried forward, noting that further development of the model may later favor either fine- or coarse-grained groups.

ASSOCIATED CONTENT

Supporting Information

The Supporting Information is available free of charge at <https://pubs.acs.org/doi/10.1021/acs.iecr.3c01548>.

Additional s-SAFT- γ Mie group interaction parameters for primary amines, alkanolamines, as well as mixtures of CO₂ with primary or secondary alcohols; additional s-SAFT- γ Mie pure component VLE descriptions of primary amines, primary and secondary alcohols, as well as binary mixture VLE descriptions of CO₂ with primary and secondary alcohols (PDF)

AUTHOR INFORMATION

Corresponding Author

Jamie T. Cripwell – Department of Chemical Engineering, Stellenbosch University, Matieland 7602, South Africa;  orcid.org/0000-0002-2439-5460; Email: cripwell@sun.ac.za

Authors

Alexander Schulze-Hulbe – Department of Chemical Engineering, Stellenbosch University, Matieland 7602, South Africa;  orcid.org/0000-0002-7935-8958

Fariborz Shaahmadi – Department of Chemical Engineering, Stellenbosch University, Matieland 7602, South Africa;  orcid.org/0000-0002-7936-0804

Andries J. Burger – Department of Chemical Engineering, Stellenbosch University, Matieland 7602, South Africa;  orcid.org/0000-0001-6588-807X

Complete contact information is available at:

<https://pubs.acs.org/10.1021/acs.iecr.3c01548>

Notes

The authors declare no competing financial interest.

ACKNOWLEDGMENTS

The financial assistance of Sasol Technology (Pty) Ltd., as well as the Wilhelm Frank foundation are hereby acknowledged. Opinions expressed and conclusions presented are those of the authors and are not necessarily to be attributed to the sponsors. The authors thank Dr S.A.M. Smith for helpful discussions.

REFERENCES

- (1) IPCC. *Climate Change 2014: Mitigation of Climate Change. Working Group III Contribution to the Fifth Assessment Report of the Intergovernmental Panel on Climate Change*; Cambridge University Press, 2014.
- (2) Bui, M.; Adjiman, C. S.; Bardow, A.; Anthony, E. J.; Boston, A.; Brown, S.; Fennell, P. S.; Fuss, S.; Galindo, A.; Hackett, L. A.; et al. Carbon Capture and Storage (CCS): The Way Forward. *Energy Environ. Sci.* **2018**, *11* (5), 1062–176.
- (3) Benhelal, E.; Zahedi, G.; Shamsaei, E.; Bahadori, A. Global Strategies and Potentials to Curb CO₂ Emissions in Cement Industry. *J. Cleaner Prod.* **2013**, *51*, 142–61.
- (4) Vrbová, V.; Ciahotný, K. Upgrading Biogas to Biomethane Using Membrane Separation. *Energy Fuels.* **2017**, *31* (9), 9393–401.
- (5) Liang, Z. H.; Rongwong, W.; Liu, H.; Fu, K.; Gao, H.; Cao, F.; Zhang, R.; Sema, T.; Henni, A.; Sumon, K.; et al. Recent Progress and New Developments in Post-Combustion Carbon-Capture Technology with Amine Based Solvents. *Int. J. Greenh. Gas Control.* **2015**, *40*, 26–54.
- (6) Papadopoulos, A. I.; Badr, S.; Chremos, A.; Forte, E.; Zarogiannis, T.; Seferlis, P.; Papadokonstantakis, S.; Galindo, A.; Jackson, G.; Adjiman, C. S. Computer-Aided Molecular Design and Selection of CO₂ Capture Solvents Based on Thermodynamics, Reactivity and Sustainability. *Mol. Syst. Des. Eng.* **2016**, *1* (3), 313–34.
- (7) Liang, Z.; Fu, K.; Idem, R.; Tontiwachwuthikul, P. Review on Current Advances, Future Challenges and Consideration Issues for Post-Combustion CO₂ Capture Using Amine-Based Absorbents. *Chin. J. Chem. Eng.* **2016**, *24* (2), 278–88.
- (8) Yu, C. H.; Huang, C. H.; Tan, C. S. A Review of CO₂ Capture by Absorption and Adsorption. *Aerosol Air Qual. Res.* **2012**, *12* (5), 745–69.
- (9) Bui, M.; Tait, P.; Lucquiaud, M.; Mac Dowell, N. Dynamic Operation and Modelling of Amine-Based CO₂ Capture at Pilot Scale. *Int. J. Greenh. Gas Control.* **2018**, *79*, 134–53.
- (10) Mondal, M. K.; Balsora, H. K.; Varshney, P. Progress and Trends in CO₂ Capture/Separation Technologies: A Review. *Energy.* **2012**, *46* (1), 431–41.
- (11) Heldebrant, D. J.; Koech, P. K.; Glezakou, V. A.; Rousseau, R.; Malhotra, D.; Cantu, D. C. Water-Lean Solvents for Post-Combustion CO₂ Capture: Fundamentals, Uncertainties, Opportunities, and Outlook. *Chem. Rev.* **2017**, *117* (14), 9594–624.
- (12) Vitillo, J. G.; Smit, B.; Gagliardi, L. Introduction: Carbon Capture and Separation. *Chem. Rev.* **2017**, *117* (14), 9521–3.
- (13) Budzianowski, W. M. Explorative Analysis of Advanced Solvent Processes for Energy Efficient Carbon Dioxide Capture by Gas-Liquid Absorption. *Int. J. Greenh. Gas Control.* **2016**, *49*, 108–20.
- (14) Lail, M.; Tanthana, J.; Coleman, L. Non-aqueous solvent (NAS) CO₂ Capture Process. *Energy Procedia.* **2014**, *63*, 580–94.
- (15) Chowdhury, F. A.; Goto, K.; Yamada, H.; Matsuzaki, Y. A Screening Study of Alcohol Solvents for Alkanolamine-based CO₂ Capture. *Int. J. Greenh. Gas Control.* **2020**, *99*, 103081.
- (16) Bahamon, D.; Alkhatab, I. I. I.; Alkhatab, N.; Builes, S.; Sinnokrot, M.; Vega, L. F. A Comparative Assessment of Emerging Solvents and Adsorbents for Mitigating CO₂ Emissions from the Industrial Sector by Using Molecular Modeling Tools. *Front. Energy Res.* **2020**, *8*, 00165.
- (17) Alkhatab, I. I. I.; Pereira, L. M. C.; Alhajaj, A.; Vega, L. F. Performance of Non-aqueous Amine Hybrid Solvent Mixtures for CO₂ Capture: A Study Using a Molecular-based Model. *J. CO₂ Util.* **2020**, *35*, 126–44.
- (18) Wanderley, R. R.; Pinto, D. D. D.; Knuutila, H. K. From Hybrid Solvents to Water-Lean Solvents – A Critical and Historical Review. *Sep. Purif. Technol.* **2021**, *260*, 118193.
- (19) Barzagli, F.; Giorgi, C.; Mani, F.; Peruzzini, M. Reversible Carbon Dioxide Capture by Aqueous and Non-Aqueous Amine-Based Adsorbents: A Comparative Analysis Carried out by ¹³C NMR Spectroscopy. *Appl. Energy.* **2018**, *220*, 208–19.
- (20) Mathias, P. M.; Reddy, S.; Smith, A.; Afshar, K. Thermodynamic Analysis of CO₂ Capture Solvents. *Int. J. Greenh. Gas Control.* **2013**, *19*, 262–70.
- (21) Barzagli, F.; Lai, S.; Mani, F.; Stoppioni, P. Novel Non-Aqueous Amine Solvents for Biogas Upgrading. *Energy Fuels.* **2014**, *28*, 5252–8.
- (22) Barzagli, F.; Mani, F.; Peruzzini, M. Efficient CO₂ Absorption and Low Temperature Desorption with Non-aqueous Solvents Based on 2-Amino-2-Methyl-1-Propanol (AMP). *Int. J. Greenh. Gas Control.* **2013**, *16*, 217–23.
- (23) Barbarossa, V.; Barzagli, F.; Mani, F.; Lai, S.; Stoppioni, P.; Vanga, G. Efficient CO₂ Capture by Non-Aqueous 2-Amino-2-Methyl-1-Propanol (AMP) and Low Temperature Solvent Regeneration. *RSC Adv.* **2013**, *3*, 12349–12355.
- (24) Mathias, P. M.; Afshar, K.; Zheng, F.; Bearden, M. D.; Freeman, C. J.; Andrea, T.; Koech, P. K.; Kutnyakov, I.; Zwoster, A.; Smith, A. R.; et al. Improving the Regeneration of CO₂-binding Organic Liquids with a Polarity Change. *Energy Environ. Sci.* **2013**, *6* (7), 2233–42.
- (25) Guo, H.; Li, C.; Shi, X.; Li, H.; Shen, S. Nonaqueous Amine-Based Adsorbents for Energy Efficient CO₂ Capture. *Appl. Energy.* **2019**, *239*, 725–34.
- (26) Wertheim, M. Fluids with Highly Directional Attractive Forces. I. Statistical Thermodynamics. *J. Stat. Phys.* **1984**, *35*, 19–34.
- (27) Wertheim, M. Fluids with Highly Directional Attractive Forces. II. Thermodynamic Perturbation Theory and Integral Equations. *J. Stat. Phys.* **1984**, *35*, 35–47.
- (28) Wertheim, M. Fluids with Highly Directional Attractive Forces. III. Multiple Attraction Sites. *J. Stat. Phys.* **1986**, *42*, 459–76.
- (29) Wertheim, M. Fluids with Highly Directional Attractive Forces. IV. Equilibrium Polymerization. *J. Stat. Phys.* **1986**, *42*, 477–92.
- (30) Tumakaka, F.; Gross, J.; Sadowski, G. Modeling of Polymer Phase Equilibria using Perturbed-Chain SAFT. *Fluid Phase Equilib.* **2002**, *194–197*, 541–51.
- (31) Kouskoumvakaki, I. A.; Von Solms, N.; Michelsen, M. L.; Kontogeorgis, G. M. Application of the Perturbed Chain SAFT

- Equation of State to Complex Polymer Systems using Simplified Mixing Rules. *Fluid Phase Equilib.* **2004**, *215*, 71–8.
- (32) Peng, Y.; Goff, K.; dos Ramos, M. C.; McCabe, C. Predicting the Phase Behavior of Polymer Systems with the GC-SAFT-VR Approach. *Ind. Eng. Chem. Res.* **2010**, *49* (3), 1378–1394.
- (33) Von Solms, N.; Michelsen, M. L.; Kontogeorgis, G. M. Prediction and Correlation of High-Pressure Gas Solubility in Polymers with Simplified PC-SAFT. *Ind. Eng. Chem. Res.* **2005**, *44* (9), 3330–5.
- (34) Peters, F. T.; Laube, F. S.; Sadowski, G. Development of a Group Contribution Method for Polymers within the PC-SAFT Model. *Fluid Phase Equilib.* **2012**, *324*, 70–9.
- (35) Tihic, A.; Kontogeorgis, G. M.; von Solms, N.; Michelsen, M. L.; Constantinou, L. A Predictive Group-Contribution Simplified PC-SAFT Equation of State: Application to Polymer Systems. *Ind. Eng. Chem. Res.* **2008**, *47* (15), 5092–5101.
- (36) Pedrosa, N.; Vega, L. F.; Coutinho, J. A. P.; Marrucho, I. M. Phase Equilibria Calculations of Polyethylene Solutions from SAFT-Type Equations of State. *Macromolecules.* **2006**, *39* (12), 4240–6.
- (37) Tihic, A.; von Solms, N.; Michelsen, M. L.; Kontogeorgis, G. M.; Constantinou, L. Application of sPC-SAFT and Group Contribution sPC-SAFT to Polymer Systems - Capabilities and Limitations. *Fluid Phase Equilib.* **2009**, *281*, 70–7.
- (38) Cameretti, L. F.; Sadowski, G.; Mollerup, J. M. Modeling of Aqueous Electrolyte Solutions with Perturbed-Chain Statistical Associated Fluid Theory. *Ind. Eng. Chem. Res.* **2005**, *44* (9), 3355–3362.
- (39) Cameretti, L.; Sadowski, G. Modeling of Aqueous Amino Acid and Polypeptide Solutions with PC-SAFT. *Chem. Eng. Process.* **2008**, *47* (6), 1018–25.
- (40) Held, C.; Reschke, T.; Mohammad, S.; Luza, A.; Sadowski, G. ePC-SAFT Revised. *Chem. Eng. Res. Des.* **2014**, *92* (12), 2884–97.
- (41) Held, C.; Reschke, T.; Müller, R.; Kunz, W.; Sadowski, G. Measuring and Modeling Aqueous Electrolyte/Amino-Acid Solutions with ePC-SAFT. *J. Chem. Thermodyn.* **2014**, *68*, 1–12.
- (42) Mohammad, S.; Grundl, G.; Müller, R.; Kunz, W.; Sadowski, G.; Held, C. Influence of Electrolytes on Liquid-Liquid Equilibria of Water/1-Butanol and on the Partitioning of 5-Hydroxymethylfurfural in Water/1-Butanol. *Fluid Phase Equilib.* **2016**, *428*, 102–11.
- (43) Pabsch, D.; Held, C.; Sadowski, G. Modeling the CO₂ Solubility in Aqueous Electrolyte Solutions Using ePC-SAFT. *J. Chem. Eng. Data* **2020**, *65* (12), 5768–77.
- (44) Llorell, F.; Marcos, R. M.; MacDowell, N.; Vega, L. F. Modeling the Absorption of Weak Electrolytes and Acid Gases with Ionic Liquids Using the Soft-SAFT Approach. *J. Phys. Chem. B* **2012**, *116* (26), 7709–18.
- (45) Galindo, A.; Gil-Villegas, A.; Jackson, G.; Burgess, A. N. SAFT-VRE: Phase Behavior of Electrolyte Solutions with the Statistical Associating Fluid Theory for Potentials of Variable Range. *J. Phys. Chem. B* **1999**, *103* (46), 10272–81.
- (46) Gil-Villegas, A.; Galindo, A.; Jackson, G. A Statistical Associating Fluid Theory for Electrolyte Solutions (SAFT-VRE). *Mol. Phys.* **2001**, *99* (6), 531–46.
- (47) Li, X. S.; Englezos, P. Vapor-Liquid Equilibrium of Systems Containing Alcohols, Water, Carbon Dioxide and Hydrocarbons Using SAFT. *Fluid Phase Equilib.* **2004**, *224* (1), 111–8.
- (48) Gross, J.; Sadowski, G. Application of the Perturbed-Chain SAFT Equation of State to Associating Systems. *Ind. Eng. Chem. Res.* **2002**, *41*, 5510–5.
- (49) Papaioannou, V.; Adjiman, C. S.; Jackson, G.; Galindo, A. Simultaneous Prediction of Vapour-Liquid and Liquid-Liquid Equilibria (VLE and LLE) of Aqueous Mixtures with the SAFT- γ Group Contribution Approach. *Fluid Phase Equilib.* **2011**, *306* (1), 82–96.
- (50) Liang, X.; Tsivintzelis, I.; Kontogeorgis, G. M. Modeling Water Containing Systems with the Simplified PC-SAFT and CPA Equations of State. *Ind. Eng. Chem. Res.* **2014**, *53* (37), 14493–507.
- (51) Cripwell, J.; Smith, S.; Schwarz, C.; Burger, A. SAFT-VR Mie: Applications to Phase Equilibria of Alcohols in Mixtures with n-Alkanes and Water. *Ind. Eng. Chem. Res.* **2018**, *57* (29), 9693–706.
- (52) Lafitte, T.; Apostolakou, A.; Avendaño, C.; Galindo, A.; Adjiman, C. S.; Müller, E. A.; Jackson, G. Accurate Statistical Associating Fluid Theory for Chain Molecules Formed from Mie Segments. *J. Chem. Phys.* **2013**, *139* (15), 154504.
- (53) Lafitte, T.; Bessières, D.; Piñeiro, M. M.; Daridon, J. L. Simultaneous Estimation of Phase Behavior and Second-Derivative Properties Using the Statistical Associating Fluid Theory with Variable Range Approach. *J. Chem. Phys.* **2006**, *124* (2), No. 024509.
- (54) Lafitte, T.; Piñeiro, M. M.; Daridon, J. L.; Bessières, D. A Comprehensive Description of Chemical Association Effects on Second Derivative Properties of Alcohols Through a SAFT-VR Approach. *J. Phys. Chem. B* **2007**, *111* (13), 3447–61.
- (55) Zhu, C.; Liu, X.; He, M.; Kontogeorgis, G. M.; Liang, X. Heat Capacities of Fluids: The Performance of Various Equations of State. *J. Chem. Eng. Data* **2020**, *65* (12), 5654–76.
- (56) Dufal, S.; Lafitte, T.; Galindo, A.; Jackson, G.; Haslam, A. J. Developing Intermolecular-Potential Models for Use with the SAFT-VR Mie Equation of State. *AIChE J.* **2015**, *61* (9), 2891–912.
- (57) Dufal, S.; Lafitte, T.; Haslam, A. J.; Galindo, A.; Clark, G. N. I.; Vega, C.; Jackson, G. The A in SAFT: Developing the Contribution of Association to the Helmholtz Free Energy within a Wertheim TPT1 Treatment of Generic Mie Fluids. *Mol. Phys.* **2015**, *113* (9–10), 948–84.
- (58) Chapman, W. G.; Gubbins, K.; Jackson, G.; Radosz, M. New Reference Equation of State for Associating Liquids. *Ind. Eng. Chem. Res.* **1990**, *29* (8), 1709–21.
- (59) Tan, S.; Adidharma, H.; Radosz, M. Recent Advances and Applications of Statistical Associating Fluid Theory. *Ind. Eng. Chem. Res.* **2008**, *47* (21), 8063–82.
- (60) Kontogeorgis, G.; Folas, G. *Thermodynamic Models for Industrial Applications*; John Wiley and Sons, 2010.
- (61) Huang, S.; Radosz, M. Equation of State for Small, Large, Polydisperse and Associating Molecules. *Ind. Eng. Chem. Res.* **1990**, *29* (11), 2284–94.
- (62) Gross, J.; Sadowski, G. Perturbed-Chain SAFT: An Equation of State Based on a Perturbation Theory for Chain Molecules. *Ind. Eng. Chem. Res.* **2001**, *40* (4), 1244–60.
- (63) von Solms, N.; Michelsen, M.; Kontogeorgis, G. Computational and Physical Performance of a Modified PC-SAFT Equation of State for Highly Asymmetric and Associating Mixtures. *Ind. Eng. Chem. Res.* **2003**, *42* (5), 1098–105.
- (64) Shaahmadi, F.; Smith, S. A. M.; Schwarz, C. E.; Burger, A. J.; Cripwell, J. T. Group-contribution SAFT Equations of State: A Review. *Fluid Phase Equilib.* **2023**, *565*, 113674.
- (65) Papaioannou, V.; Lafitte, T.; Avendaño, C.; Adjiman, C. S.; Jackson, G.; Müller, E. A.; Galindo, A. Group Contribution Methodology Based on the Statistical Associating Fluid Theory for Heteronuclear Molecules Formed from Mie Segments. *J. Chem. Phys.* **2014**, *140* (5), No. 054107.
- (66) Haslam, A. J.; González-Pérez, A.; Di Lecce, S.; Khalit, S. H.; Perdomo, F. A.; Kournopoulos, S.; Kohns, M.; Lindeboom, T.; Wehbe, M.; Febra, S.; et al. Expanding the Applications of the SAFT- γ Mie Group-Contribution Equation of State: Prediction of Thermodynamic Properties and Phase Behavior of Mixtures. *J. Chem. Eng. Data* **2020**, *65* (12), 5862–90.
- (67) Hutacharoen, P.; Dufal, S.; Papaioannou, V.; Shanker, R. M.; Adjiman, C. S.; Jackson, G.; Galindo, A. Predicting the Solvation of Organic Compounds in Aqueous Environments: From Alkanes and Alcohols to Pharmaceuticals. *Ind. Eng. Chem. Res.* **2017**, *56* (38), 10856–76.
- (68) Febra, S. A.; Bernet, T.; Mack, C.; McGinty, J.; Onyemelukwe, I. I.; Urwin, S. J.; Sefcik, J.; ter Horst, J. H.; Adjiman, C. S.; Jackson, G.; et al. Extending the SAFT- γ Mie Approach to Model Benzoic Acid, Diphenylamine, and Mefenamic Acid: Solubility Prediction and Experimental Measurement. *Fluid Phase Equilib.* **2021**, *540*, 113002.

- (69) Perdomo, F. A.; Khalit, S. H.; Graham, E. J.; Tzirakis, F.; Papadopoulos, A. I.; Tsivintzelis, I.; Seferlis, P.; Adjiman, C. S.; Jackson, G.; Galindo, A. A Predictive Group Contribution Framework for the Thermodynamic Modelling of CO₂ Absorption in Cyclic Amines, Alkyl Polyamines, Alkanolamines and Phase-change Amines: New Data and SAFT- γ Mie Parameters. *Fluid Phase Equilib.* **2023**, *566*, 113635.
- (70) Shaahmadi, F.; Hurter, R. M.; Cripwell, J. T.; Burger, A. J. Improving the SAFT- γ Mie Equation of State to Account for Functional Group Interactions in a Structural (s-SAFT- γ Mie) Framework: Linear & Branched Alkanes. *J. Chem. Phys.* **2021**, *154* (24), 244102.
- (71) Schulze-Hulbe, A.; Shaahmadi, F.; Burger, A. J.; Cripwell, J. T. Extending the Structural (s)-SAFT- γ Mie Equation of State to Primary Alcohols. *Ind. Eng. Chem. Res.* **2022**, *61* (33), 12208–28.
- (72) Papadopoulos, A. I.; Perdomo, F. A.; Tzirakis, F.; Shavalieva, G.; Tsivintzelis, I.; Kazepidis, P.; Nessi, E.; Papadokonstantakis, S.; Seferlis, P.; Galindo, A.; et al. Molecular Engineering of Sustainable Phase-change Solvents: From Digital Design to Scaling-up for CO₂ Capture. *Chem. Eng. J.* **2021**, *420*, 127624.
- (73) Mac Dowell, N.; Llorell, F.; Adjiman, C. S.; Jackson, G.; Galindo, A. Modeling the Fluid Phase Behavior of Carbon Dioxide in Aqueous Solutions of Monoethanolamine Using Transferable Parameters with the SAFT-VR Approach. *Ind. Eng. Chem. Res.* **2010**, *49* (4), 1883–99.
- (74) Mac Dowell, N.; Pereira, F. E.; Llorell, F.; Blas, F. J.; Adjiman, C. S.; Jackson, G.; Galindo, A. Transferable SAFT-VR Models for the Calculation of the Fluid Phase Equilibria in Reactive Mixtures of Carbon Dioxide, Water, and n-Alkylamines in the Context of Carbon Capture. *J. Phys. Chem. B* **2011**, *115* (25), 8155–68.
- (75) Rodriguez, J.; Mac Dowell, N.; Llorell, F.; Adjiman, C. S.; Jackson, G.; Galindo, A. Modelling the Fluid Phase Behaviour of Aqueous Mixtures of Multifunctional Alkanolamines and Carbon Dioxide Using Transferable Parameters with the SAFT-VR Approach. *Mol. Phys.* **2012**, *110* (11–12), 1325–48.
- (76) Gil-Villegas, A.; Galindo, A.; Whitehead, P. J.; Mills, S. J.; Jackson, G.; Burgess, A. N. Statistical Associating Fluid Theory for Chain Molecules with Attractive Potentials of Variable Range. *J. Chem. Phys.* **1997**, *106* (10), 4168–86.
- (77) Chremos, A.; Forte, E.; Papaioannou, V.; Galindo, A.; Jackson, G.; Adjiman, C. S. Modelling the Phase and Chemical Equilibria of Aqueous Solutions of Alkanolamines and Carbon Dioxide using the SAFT- γ SW Group Contribution Approach. *Fluid Phase Equilib.* **2016**, *407*, 280–97.
- (78) Khalit, S. H. Development of SAFT- γ Mie Models for Alkanolamines for Carbon Capture Studies. Ph.D. Dissertation, Imperial College London, London, U.K., 2019.
- (79) Economou, I. G.; Donohue, M. D. Chemical, Quasi-Chemical and Perturbation Theories for Associating Fluids. *AIChE J.* **1991**, *37* (12), 1875–94.
- (80) Renon, H.; Prausnitz, J. M. Local Compositions in Thermodynamic Excess Functions for Liquid Mixtures. *AIChE J.* **1968**, *14* (1), 135–44.
- (81) Pereira, L. M. C.; Llorell, F.; Vega, L. F. Thermodynamic Characterisation of Aqueous Alkanolamine and Amine Solutions for Acid Gas Processing by Transferable Molecular Models. *Appl. Energy.* **2018**, *222*, 687–703.
- (82) Pereira, L. M. C.; Vega, L. F. A Systematic Approach for the Thermodynamic Modelling of CO₂-amine Absorption Process using Molecular-Based Models. *Appl. Energy.* **2018**, *232*, 273–91.
- (83) Lloret, J. O.; Vega, L. F.; Llorell, F. A Consistent and Transferable Thermodynamic Model to Accurately Describe CO₂ Capture with Monoethanolamine. *J. CO₂ Util.* **2017**, *21*, 521–33.
- (84) Pahlavanzadeh, H.; Fakouri Baygi, S. Modeling CO₂ Solubility in Aqueous Methylidethanolamine Solutions by Perturbed Chain-SAFT Equation of State. *J. Chem. Thermodyn.* **2013**, *59*, 214–21.
- (85) Fakouri Baygi, S.; Pahlavanzadeh, H. Application of the Perturbed Chain-SAFT Equation of State for Modeling CO₂ Solubility in Aqueous Monoethanolamine Solutions. *Chem. Eng. Res. Des.* **2015**, *93*, 789–99.
- (86) Najafloo, A.; Feyzi, F.; Zoghi, A. T. Modeling Solubility of CO₂ in Aqueous MDEA Solution Using Electrolyte SAFT-HR EoS. *J. Taiwan Inst. Chem. Eng.* **2016**, *58*, 381–90.
- (87) Najafloo, A.; Zarei, S. Modeling Solubility of CO₂ in Aqueous Monoethanolamine (MEA) Solution using SAFT-HR Equation of State. *Fluid Phase Equilib.* **2018**, *456*, 25–32.
- (88) Blas, F. J.; Vega, L. F. Thermodynamic Behaviour of Homonuclear and Heteronuclear Lennard-Jones Chains with Association Sites from Simulation and Theory. *Mol. Phys.* **1997**, *92* (1), 135–50.
- (89) Blas, F. J.; Vega, L. F. Critical Behavior and Partial Miscibility Phenomena in Binary Mixtures of Hydrocarbons by the Statistical Associating Fluid Theory. *J. Chem. Phys.* **1998**, *109* (17), 7405–13.
- (90) Blas, F. J.; Vega, L. F. Prediction of Binary and Ternary Diagrams using the Statistical Associating Fluid Theory (SAFT) Equation of State. *Ind. Eng. Chem. Res.* **1998**, *37* (2), 660–74.
- (91) Alkhatab, I. I. I.; Galindo, A.; Vega, L. F. Systematic Study of the Effect of the Co-solvent on the Performance of Amine-based Solvents for CO₂ Capture. *Sep. Purif. Technol.* **2022**, *282*, 120093.
- (92) Kontogeorgis, G. M.; Dohrn, R.; Economou, I. G.; de Hemptinne, J. C.; ten Kate, A.; Kuitunen, S.; Mooijer, M.; Zilnik, L. F.; Vesovic, V. Industrial Requirements for Thermodynamic and Transport Properties: 2020. *Ind. Eng. Chem. Res.* **2021**, *60* (13), 4987–5013.
- (93) Dufal, S.; Papaioannou, V.; Sadeqzadeh, M.; Pogiatzis, T.; Chremos, A.; Adjiman, C. S.; Jackson, G.; Galindo, A. Prediction of Thermodynamic Properties and Phase Behavior of Fluids and Mixtures with the SAFT- γ Mie Group-Contribution Equation of State. *J. Chem. Eng. Data* **2014**, *59* (10), 3272–88.
- (94) Sadeqzadeh, M.; Papaioannou, V.; Dufal, S.; Adjiman, C. S.; Jackson, G.; Galindo, A. The Development of Unlike Induced Association-Site Models to Study the Phase Behaviour of Aqueous Mixtures Comprising Acetone, Alkanes and Alkyl Carboxylic Acids with the SAFT-g Mie Group Contribution Methodology. *Fluid Phase Equilib.* **2016**, *407*, 39–57.
- (95) Papaioannou, V.; Calado, F.; Lafitte, T.; Dufal, S.; Sadeqzadeh, M.; Jackson, G.; Adjiman, C. S.; Galindo, A. Application of the SAFT- γ Mie Group Contribution Equation of State to Fluids of Relevance to the Oil and Gas Industry. *Fluid Phase Equilib.* **2016**, *416*, 104–19.
- (96) Grandjean, L.; de Hemptinne, J.-C.; Lugo, R. Application of GC-PPC-SAFT EoS to Ammonia and its Mixtures. *Fluid Phase Equilib.* **2014**, *367*, 159–172.
- (97) Dominik, A.; Chapman, W. G.; Kleiner, M.; Sadowski, G. Modeling of Polar Systems with the Perturbed-Chain SAFT Equation of State. Investigation of the Performance of Two Polar Terms. *Ind. Eng. Chem. Res.* **2005**, *44* (17), 6928–38.
- (98) de Villiers, A. J.; Schwarz, C. E.; Burger, A. J. Improving Vapour-Liquid-Equilibria Predictions for Mixtures with Non-Associating Polar Components Using sPC-SAFT Extended with Two Dipolar Terms. *Fluid Phase Equilib.* **2011**, *305*, 174–84.
- (99) de Villiers, A. J.; Schwarz, C. E.; Chobanov, K. G.; Burger, A. J. Application of sPC-SAFT-JC and sPC-SAFT-GV to Phase Equilibria Predictions of Alkane/Alcohol, Alcohol/Alcohol, and Water/Alcohol Binary Systems. *Ind. Eng. Chem. Res.* **2014**, *53* (14), 6065–75.
- (100) Cripwell, J. T.; Schwarz, C. E.; Burger, A. J. Polar (s)PC-SAFT: Modelling of Polar Structural Isomers and Identification of the Systematic Nature of Regression Issues. *Fluid Phase Equilib.* **2017**, *449*, 156–66.
- (101) Tybjerg, P. C. V.; Kontogeorgis, G. M.; Michelsen, M. L.; Stenby, E. H. Phase Equilibria Modeling of Methanol-containing Systems with the CPA and sPC-SAFT Equations of State. *Fluid Phase Equilib.* **2010**, *288*, 128–38.
- (102) de Villiers, A. J.; Schwarz, C. E.; Burger, A. J.; Kontogeorgis, G. M. Evaluation of the PC-SAFT, SAFT and CPA Equations of State in Predicting Derivative Properties of Selected Non-polar and Hydrogen-bonding Compounds. *Fluid Phase Equilib.* **2013**, *338*, 1–15.

- (103) Hurter, R.; Cripwell, J.; Burger, A. Expanding SAFT- γ Mie's Application to Dipolar Species: 2-Ketones, 3-Ketones and Propanoate Esters. *Ind. Eng. Chem. Res.* **2020**, *59* (16), 7993–8003.
- (104) Cripwell, J. T.; Kruger, F. J.; Burger, A. J. Accounting for Cross Association in Non-self-associating Species Using a Physically Consistent SAFT-VR Mie Approach. *Fluid Phase Equilib.* **2019**, *483*, 1–13.
- (105) Wu, H. S.; Sandler, S. I. Use of ab Initio Quantum Mechanics Calculations in Group Contribution Methods. 1. Theory and the Basis for Group Identifications. *Ind. Eng. Chem. Res.* **1991**, *30* (5), 881–9.
- (106) Perdomo, F. A.; Khalit, S. H.; Adjiman, C. S.; Galindo, A.; Jackson, G. Description of the Thermodynamic Properties and Fluid-Phase Behavior of Aqueous Solutions of Linear, Branched, and Cyclic Amines. *AICHE J.* **2021**, *67* (3), e17194.
- (107) Grenner, A.; Schmelzer, J.; Von Solms, N.; Kontogeorgis, G. M. Comparison of Two Association Models (Elliott-Suresh-Donohue and Simplified PC-SAFT) for Complex Phase Equilibria of Hydrocarbon-Water and Amine-Containing Mixtures. *Ind. Eng. Chem. Res.* **2006**, *45* (24), 8170–9.
- (108) Lymeriadis, A.; Adjiman, C.; Jackson, G.; Galindo, A. A Generalisation of the SAFT- γ Group Contribution Method for Groups Comprising Multiple Spherical Segments. *Fluid Phase Equilib.* **2008**, *274*, 85–104.
- (109) Kaarsholm, M.; Derawi, S. O.; Michelsen, M. L.; Kontogeorgis, G. M. Extension of the Cubic-plus-Association (CPA) Equation of State to Amines. *Ind. Eng. Chem. Res.* **2005**, *44*, 4406–13.
- (110) Rozmus, J.; de Hemptinne, J.-C.; Mougin, P. Application of GC-PPC-SAFT EoS to Amine Mixtures with a Predictive Approach. *Fluid Phase Equilib.* **2011**, *303*, 15–30.
- (111) Rozmus, J.; de Hemptinne, J.-C.; Ferrando, N.; Mougin, P. Long Chain Multifunctional Molecules with GC-PPC-SAFT: Limits of Data and Model. *Fluid Phase Equilib.* **2012**, *329*, 78–85.
- (112) dos Ramos, M. C.; Haley, J. D.; Westwood, J. R.; McCabe, C. Extending the GC-SAFT-VR Approach to Associating Functional Groups: Alcohols, Aldehydes, Amines and Carboxylic Acids. *Fluid Phase Equilib.* **2011**, *306*, 97–111.
- (113) Perdomo, F. A.; Millán, B. M.; Aragón, J. L. Predicting the Physical-chemical Properties of Biodiesel Fuels Assessing the Molecular Structure with the SAFT- γ Group Contribution Approach. *Energy* **2014**, *72*, 274–290.
- (114) Nguyenhuynh, D.; Tran, S. T. K.; Mai, C. T. Q. Predicting the Phase Behavior of Alcohols, Aromatic Alcohols, and Their Mixtures using the Modified Group-Contribution Perturbed-Chain Statistical Associating Fluid Theory. *Ind. Eng. Chem. Res.* **2019**, *58* (36), 16963–77.
- (115) Susial Badajoz, P.; García-Montesdeoca, I.; García-Vera, D.; Marrero-Perez, A.; Herrera-Vega, P.; Calvo-Castillo, L. PC-SAFT Modeling of the High Pressure VLE data for 2,2,4-Trimethylpentane with Ethanol, 1-Propanol, 2-Propanol and 1-Butanol. Experimental Equipment and Binary Systems at 1.5 MPa. *J. Chem. Thermodyn.* **2022**, *172*, 106816.
- (116) Shirazi, S. G.; Kermanpour, F. Thermodynamic Study of Binary Mixture of 2-Butanol + Monoethanolamine at Different Temperatures; PC-SAFT and ERAS models. *J. Mol. Liq.* **2020**, *320*, 114461.
- (117) Reilly, J. T.; Bokis, C. P.; Donohue, M. D. An Experimental Investigation of Lewis Acid-Base Interactions of Liquid Carbon Dioxide using Fourier Transform Infrared (FT-IR) spectroscopy. *Int. J. Thermophys.* **1995**, *16*, 599–610.
- (118) Smith, S. A.; Cripwell, J. T.; Schwarz, C. E. A Quadrupolar SAFT-VR Mie Approach to Modeling Binary Mixtures of CO₂ or Benzene with n-Alkanes or 1-Alkanols. *J. Chem. Eng. Data* **2020**, *65* (12), 5778–800.
- (119) NguyenHuynh, D.; Passarello, J. P.; De Hemptinne, J. C.; Volle, F.; Tobaly, P. Simultaneous Modeling of VLE, LLE and VLLE of CO₂ and 1, 2, 3 and 4 Alkanol Containing Mixtures using GC-PPC-SAFT EOS. *J. Supercrit. Fluids* **2014**, *95*, 146–57.
- (120) Bjørner, M. G.; Kontogeorgis, G. M. Modeling Derivative Properties and Binary Mixtures with CO₂ using the CPA and the Quadrupolar CPA Equations of State. *Fluid Phase Equilib.* **2016**, *408*, 151–169.
- (121) Ramírez-Vélez, N.; Piña-Martinez, A.; Jaubert, J. N.; Privat, R. Parameterization of SAFT Models: Analysis of Different Parameter Estimation Strategies and Application to the Development of a Comprehensive Database of PC-SAFT Molecular Parameters. *J. Chem. Eng. Data* **2020**, *65* (12), 5920–32.
- (122) Wilding, W. V.; Knotts, T. A.; Giles, N. F.; Rowley, R. L. *DIPPR Data Compilation of Pure Chemical Properties*; Design Institute for Physical Properties, AIChE: New York, NY, 2020.
- (123) Wilding, W. V.; Knotts, T. A.; Giles, N. F.; Rowley, R. L. *DIPPR Data Compilation of Pure Chemical Properties*; Design Institute for Physical Properties, AIChE: New York, NY, 2022.
- (124) Levenberg, K. A Method for the Solution of Certain Non-Linear Problems in Least Squares. *Q. Appl. Math.* **1944**, *2* (2), 164–8.
- (125) Marquardt, D. W. An Algorithm for Least-Squares Estimation of Nonlinear Parameters. *J. Soc. Ind. Appl. Math.* **1963**, *11* (2), 431–41.
- (126) Letcher, T. M.; Bayles, J. W. Thermodynamics of Some Binary Liquid Mixtures Containing Aliphatic Amines. *J. Chem. Eng. Data* **1971**, *16* (3), 266–71.
- (127) Wolfová, J.; Linek, J.; Wichterle, I. Vapour-Liquid Equilibria in the Heptane - 2-Pentanol and Heptane - 2-Methyl-1-Butanol Systems at 75, 85 and 95°C. *Fluid Phase Equilib.* **1991**, *64*, 281–9.
- (128) Brown, T. S.; Niesen, V. G.; Sloan, E. D.; Kidnay, A. J. Vapour-Liquid Equilibria for the Binary System of Nitrogen, Carbon Dioxide, and n-Butane at Temperatures from 220 to 344 K. *Fluid Phase Equilib.* **1989**, *53*, 7–14.
- (129) Ohgaki, K.; Katayama, T. Isothermal Vapor-Liquid Equilibrium Data for Binary Systems Containing Carbon Dioxide at High Pressures: Methanol–Carbon Dioxide, n-Hexane–Carbon Dioxide, and Benzene–Carbon Dioxide Systems. *J. Chem. Eng. Data* **1976**, *21* (1), 53–5.
- (130) Chang, C. J.; Day, C.-Y.; Ko, C.-M.; Chiu, K.-L. Densities and P-x-y Diagrams for Carbon Dioxide Dissolution in Methanol, Ethanol and Acetone Mixtures. *Fluid Phase Equilib.* **1997**, *131*, 243–58.
- (131) Secuianu, C.; Feroiu, V.; Geana, D. High-Pressure Vapor-Liquid Equilibria in the System Carbon Dioxide and 2-Propanol at Temperatures from 293.25 to 323.15 K. *J. Chem. Eng. Data* **2003**, *48*, 1384–6.
- (132) Gordon, A. J.; Ford, R. A. *Chemist's Companion - A Handbook of Practical Data, Techniques, and References*; John Wiley and Sons, 1972.
- (133) Mato, M. M.; Cebreiro, S. M.; Legido, J. L.; Paz Andrade, M. I. Study of the Effect of Increasing the Chain Length of the Alkane in Excess Molar Enthalpies of Mixtures Containing Methyl Tert-Butyl Ether, 1-Propanol, Alkane. *Fluid Phase Equilib.* **2008**, *271* (1–2), 6–12.
- (134) Kirss, H.; Kuus, M.; Siimer, E.; Kudryavtseva, L. Excess Enthalpies of 1-Butanol-2-Butanol-n-Heptane, 1-Hexanol-Cyclohexanol-n-Nonane, 2-Butanol-n-Heptane, 1-Hexanol-Cyclohexanol and Cyclohexanol-n-Nonane at 298.15 K. *Thermochim. Acta* **1995**, *255*, 63–9.
- (135) Dominguez, M.; Mainar, A. M.; Artigas, H.; Royo, F. M.; Urieta, J. S. Isobaric VLE Data of the Ternary System (1-Butanol+n-Hexane+1-Butylamine) and the Three Constituent Binary Mixtures at 101.3 kPa. *J. Chem. Eng. Jpn.* **1997**, *30* (3), 484–90.
- (136) Kern, M.; Abello, L.; Caceres, D.; Pannetier, G. The N-H···N Bond. XIV. Thermodynamic Study of the Self Association of Hexylamine. Self Association Bonding Energy of Cyclohexylamine and of Normal Hexylamine. *Bull. Soc. Chim. Fr.* **1970**, 3849.
- (137) Velasco, I.; Otin, S.; Gutiérrez Losa, C. Excess Enthalpies of Some Aliphatic Amine + n-Hexane or Benzene Mixtures. *J. Chim. Phys.* **1978**, *75*, 706–708.
- (138) Fernández, J.; Velasco, I.; Otin, S. Excess Enthalpies of Some Alkylamine (C₃-C₁₅) + Hexane, + Dodecane, or + Hexadecane Mixtures. *Int. DATA Ser., Sel. Data Mix. Ser. A* **1987**, *15*, 205–228.

- (139) Sarmiento, F.; Paz Andrade, M. I.; Fernández, J.; Bravo, R.; Pintos, M. Excess Enthalpies of 1-Heptanol + n-Alkane and Di-n-Propylamine + Normal Alcohol Mixtures at 298. 15 K. *J. Chem. Eng. Data*. **1985**, *30* (3), 321–3.
- (140) Paz-Ramos, C.; Cerdeirinha, C. A.; Costas, M. Energetic, Entropic, and Volumetric Effects in Nonaqueous Associated Solutions. *J. Phys. Chem. B* **2011**, *115* (31), 9626–33.
- (141) Papaioannou, V. A Molecular-Based Group Contribution Equation of State for the Description of Fluid Phase Behaviour and Thermodynamic Derivative Properties of Mixtures (SAFT- γ Mie). Ph.D. Thesis, Imperial College London, London, U.K., 2013.
- (142) Bara, J. What Chemicals Will We Need to Capture CO₂? *Greenh. Gases Sci. Technol.* **2012**, *2*, 162–71.
- (143) Lepaumier, H.; Picq, D.; Carrette, P. L. Degradation Study of New Solvents for CO₂ Capture in Post-Combustion. *Energy Procedia*. **2009**, *1* (1), 893–900.
- (144) Cripwell, J.; Schwarz, C.; Burger, A. SAFT-VR-Mie with an Incorporated Polar Term for Accurate Holistic Prediction of the Thermodynamic Properties of Polar Components. *Fluid Phase Equilibr.* **2018**, *455*, 24–42.
- (145) Wójcicka, M. K.; Kalinowska, B. Excess Enthalpy and Heat Capacities of Isomeric Butanols with n-Heptane at High Dilutions. *Bull. Acad. Polym. Sci.* **1977**, *25* (8), 639–647.
- (146) Palombo, F.; Tassaing, T.; Dantén, Y.; Besnard, M. Hydrogen Bonding in Liquid and Supercritical 1-Octanol and 2-Octanol Assessed by Near and Midinfrared Spectroscopy. *J. Chem. Phys.* **2006**, *125* (9), No. 094503.
- (147) Palombo, F.; Sassi, P.; Paolantoni, M.; Morresi, A.; Cataliotti, R. S. Comparison of Hydrogen Bonding in 1-Octanol and 2-Octanol as Probed by Spectroscopic Techniques. *J. Phys. Chem. B* **2006**, *110* (36), 18017–25.
- (148) Babamohammadi, S.; Shamiri, A.; Nejad Ghaffar Borhani, T.; Shafeeyan, M. S.; Aroua, M. K.; Yusoff, R. Solubility of CO₂ in Aqueous Solutions of Glycerol and Monoethanolamine. *J. Mol. Liq.* **2018**, *249*, 40–52.
- (149) Valeh-e-Sheyda, P.; Barati, J. Mass Transfer Performance of Carbon Dioxide Absorption in a Packed Column Using Monoethanolamine-Glycerol as a Hybrid Solvent. *Process Saf. Environ. Prot.* **2021**, *146*, 54–68.
- (150) Babamohammadi, S.; Yusoff, R.; Aroua, M. K.; N. Borhani, T. Mass Transfer Coefficients of Carbon Dioxide in Aqueous Blends of Monoethanolamine and Glycerol Using Wetted-Wall Column. *J. Environ. Chem. Eng.* **2021**, *9* (6), 106618.
- (151) Shamiri, A.; Shafeeyan, M. S.; Tee, H. C.; Leo, C. Y.; Aroua, M. K.; Aghamohammadi, N. Absorption of CO₂ into Aqueous Mixtures of Glycerol and Monoethanolamine. *J. Nat. Gas Sci. Eng.* **2016**, *35*, 605–13.
- (152) Mirzaei, S.; Shamiri, A.; Aroua, M. K. Simulation of Aqueous Blend of Monoethanolamine and Glycerol for Carbon Dioxide Capture from Flue Gas. *Energy Fuels.* **2016**, *30* (11), 9540–53.
- (153) Aschenbrenner, O.; Styring, P. Comparative Study of Solvent Properties for Carbon Dioxide Absorption. *Energy Environ. Sci.* **2010**, *3*, 1106–13.
- (154) Marshall, B. D.; Chapman, W. G. Resummed Thermodynamic Perturbation Theory for Bond Cooperativity in Associating Fluids. *J. Chem. Phys.* **2013**, *139* (21), 214106.
- (155) Jahn, D. A.; Akinkunmi, F. O.; Giovambattista, N. Effects of Temperature on the Properties of Glycerol: A Computer Simulation Study of Five Different Force Fields. *J. Phys. Chem. B* **2014**, *118* (38), 11284–94.
- (156) Hiaki, T.; Taniguchi, A.; Tsuji, T.; Hongo, M. Isothermal Vapor-Liquid Equilibria of Octane with 1-Butanol, 2-Butanol, or 2-Methyl-2-Propanol. *Fluid Phase Equilib.* **1998**, *144* (1–2), 145–55.
- (157) Ortega, J. International DATA Series. *Int. DATA Ser., Sel. Data Mixtures, Ser. A* **1990**, *18* (2), 94–110.
- (158) Brown, I.; Fock, W.; Smith, F. The Thermodynamic Properties of Solutions of Normal and Branched Alcohols in Benzene and n-Hexane. *J. Chem. Thermodyn.* **1969**, *1* (3), 273–91.
- (159) Diky, V.; Muzny, C.; Smolyanitsky, A.; Bazyleva, A.; Chirico, R.; Magee, J.; Paulechka, Y.; Kazakov, A.; Townsend, S.; Lemmon, E.; et al. *ThermoData Engine (TDE) (Pure Compounds, Binary Mixtures, Ternary Mixtures, and Chemical Reactions): NIST Standard Reference Database 103b*, Version 10.1; National Institute of Standards and Technology, Standard Reference Program: Gaithersburg, MD, 2016.
- (160) Linek, J.; Wichterle, I. Isobaric Vapor-Liquid Equilibria in Six Binary Systems Containing Hexane + a Pentanol Isomer at 27, 53, and 93 kPa. *Int. Electron. J. Phys.-Chem. Data*. **1995**, *4*, 265–274.
- (161) Crespo, E. A.; Coutinho, J. A. P. Insights into the Limitations of Parameter Transferability in Heteronuclear SAFT-type Equations of State. *arXiv (Condensed Matter, Statistical Mechanics)*, November 8, 2022, 2211.04606, ver. 1. DOI: [10.48550/arXiv.2211.04606](https://doi.org/10.48550/arXiv.2211.04606) (accessed January 10, 2023).
- (162) Nagahama, K.; Hoshino, D.; Hirata, M.; Konishi, H. Binary Vapor-Liquid Equilibria of Carbon Dioxide-Light Hydrocarbons at Low Temperature. *J. Chem. Eng. Jpn.* **1974**, *7* (5), 323–8.
- (163) Cheng, H.; Pozo de Fernández, M.; Zollweg, J. A.; Streett, W. B. Vapor-Liquid Equilibrium in the System Carbon Dioxide + n-Pentane from 252 to 458 K at Pressures to 10 MPa. *J. Chem. Eng. Data* **1989**, *34*, 319–23.
- (164) McCabe, C.; Kiselev, S. B. Application of Crossover Theory to the SAFT-VR Equation of State: SAFT-VRX for Pure Fluids. *Ind. Eng. Chem. Res.* **2004**, *43* (11), 2839–51.
- (165) Aaron, D.; Tsouris, C. Separation of CO₂ from Flue Gas: A Review. *Sep. Sci. Technol.* **2005**, *40* (1–3), 321–48.
- (166) van Konynenburg, P. H.; Scott, R. L. Critical Lines and Phase Equilibria in Binary Van Der Waals Mixtures. *Philos. Trans. R. Soc., A* **1980**, *298* (1442), 495–540.
- (167) Llovel, F.; Vega, L. F. Global Fluid Phase Equilibria and Critical Phenomena of Selected Mixtures using the Crossover soft-SAFT Equation. *J. Phys. Chem. B* **2006**, *110* (3), 1350–62.
- (168) Secuianu, C.; Feroiu, V.; Geană, D. High-Pressure Phase Equilibria in the (Carbon Dioxide + 1-Hexanol) System. *J. Chem. Thermodyn.* **2010**, *42*, 1286–91.
- (169) Raeissi, S.; Gautier, K.; Peters, C. J. Fluid Multiphase Behavior in Quasi-Binary Mixtures of Carbon Dioxide and Certain 1-Alkanols. *Fluid Phase Equilib.* **1998**, *147* (1–2), 239–49.
- (170) Secuianu, C.; Feroiu, V.; Geană, D. Phase Behavior for Carbon Dioxide + Ethanol System: Experimental Measurements and Modeling with a Cubic Equation of State. *J. Supercrit. Fluids*. **2008**, *47*, 109–116.
- (171) Secuianu, C.; Feroiu, V.; Geană, D. High-Pressure Phase Equilibria for the Carbon Dioxide + 1-Propanol System. *J. Chem. Eng. Data* **2008**, *53*, 2444–8.
- (172) Tian, Y.; Chen, L.; Li, M.; Fu, H. Calculation of Gas - Liquid Critical Curves for Carbon Dioxide - 1-Alkanol Binary Systems. *J. Phys. Chem. A* **2003**, *107*, 3076–80.
- (173) Byun, H. S.; Kwak, C. High Pressure Phase Behavior for Carbon Dioxide-1-Butanol and Carbon Dioxide-1-Octanol Systems. *Korean J. Chem. Eng.* **2002**, *19* (6), 1007–13.
- (174) Lam, D. H.; Jangkamolkulchai, A.; Luks, K. D. Liquid-Liquid-Vapor Phase Equilibrium Behavior of Certain Binary Carbon Dioxide + n-Alkanol Mixtures. *Fluid Phase Equilib.* **1990**, *60*, 131–41.
- (175) Polishuk, I.; Wisniak, J.; Segura, H.; Yelash, L. V.; Kraska, T. Prediction of the Critical Locus in Binary Mixtures Using Equation of State II. Investigation of van der Waals-Type and Carnahan – Starling-Type Equations of State. *Fluid.* **2000**, *172*, 1–26.
- (176) Secuianu, C.; Feroiu, V.; Geana, D. Phase Behavior for the Carbon Dioxide + 2-Butanol System: Experimental Measurements and Modeling with Cubic Equations of State. *J. Chem. Eng. Data* **2009**, *54*, 1493–9.
- (177) Bejarano, A.; Gutiérrez, J. E.; Araus, K. A.; De La Fuente, J. C. Measurement and Modeling of High-Pressure (Vapor+Liquid) Equilibria of (CO₂+Alkanol) Binary Systems. *J. Chem. Thermodyn.* **2011**, *43* (5), 759–63.
- (178) Carissimi, G.; Montalbán, M. G.; Díaz Baños, F. G.; Villora, G. High Pressure Phase Equilibria for Binary Mixtures of CO₂ + 2-

Pentanol, Vinyl Butyrate, 2-Pentyl Butyrate or Butyric Acid Systems. *J. Supercrit. Fluids.* 2018, 135, 69–77.

(179) Sima, S.; Racoviță, R. C.; Dincă, C.; Feroiu, V. Phase Equilibria Calculations for Carbon Dioxide + 2-Propanol System. *U.P.B. Sci. Bull., Ser. B* 2017, 79 (4), 12–24.

(180) Stevens, R. M. M.; Van Roermund, J. C.; Jager, M. D.; De Loos, T. W.; De Swaan Arons, J. High-Pressure Vapour-Liquid Equilibria in the Systems Carbon Dioxide + 2-Butanol, + 2-Butyl Acetate, + Vinyl Acetate and Calculations with Three EOS Methods. *Fluid Phase Equilib.* 1997, 138 (1–2), 159–78.